

International Conference on Flow Physics and its Simulation
–In memory of Prof. Jaw-Yen Yang

New aspects of the friction of finite dry granular mass

楊馥菱 Fu-Ling Yang

fulingyang@ntu.edu.tw

Solid-Liquid Two-Phase Flow Lab

Mechanical Engineering

National Taiwan University

(NTU, Dec03-05, 2016)

Prevalence of granular flows (flows of discrete solid objects)

Nature hazards

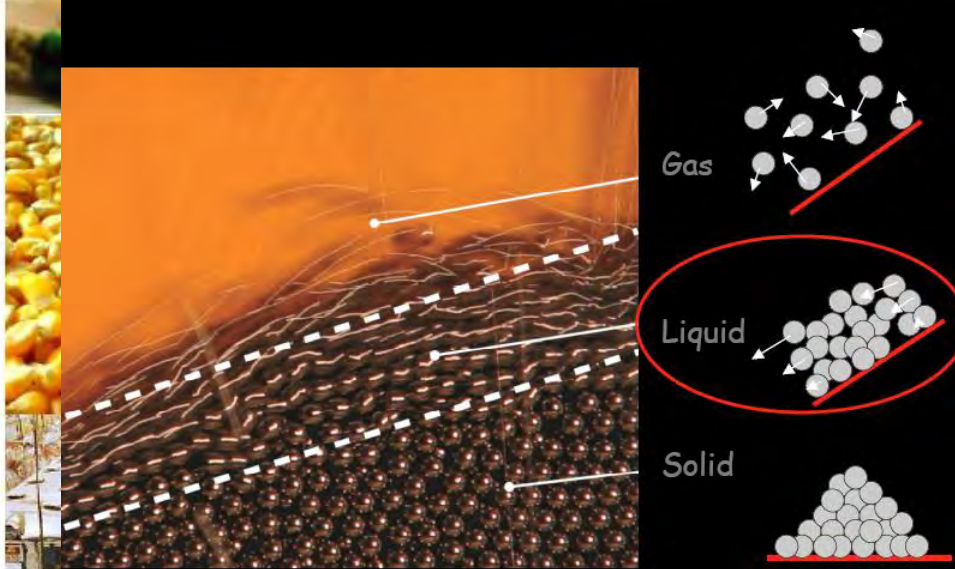


Industrial/engineering processes



Prediction / control: effective continuum model
constitutive relation + boundary condition

Granular material & its complex phasic features



Granular gas:
short **collision** dominated
“Rapid granular flow”
Kinetic Theory

Granular solid:
enduring contacts (force chains)
friction dominated
“Mohr-Coulomb continuum”
“Soil mechanics”

Granular liquid or ‘dense’ granular flow: collision + friction

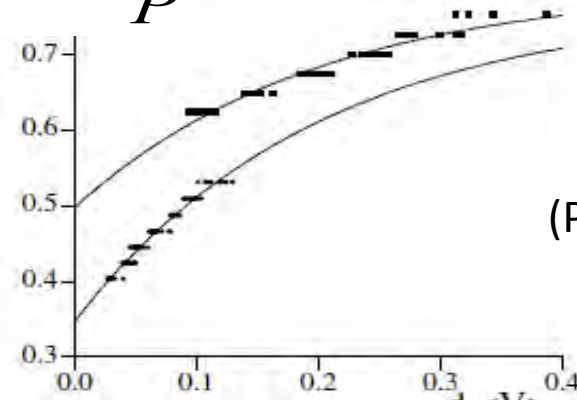
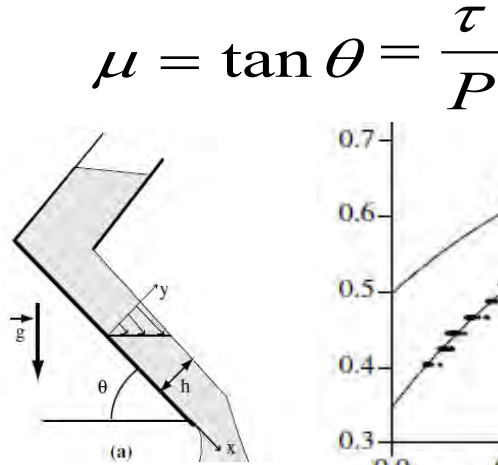
- Superposition as a complex fluid (Bingham, viscoplastic ..)
- statistical treatment (glassy material)
- phenomenological relation**

Effective friction coefficient

Treated as a solid (dense nature)

Free surface flow experiment

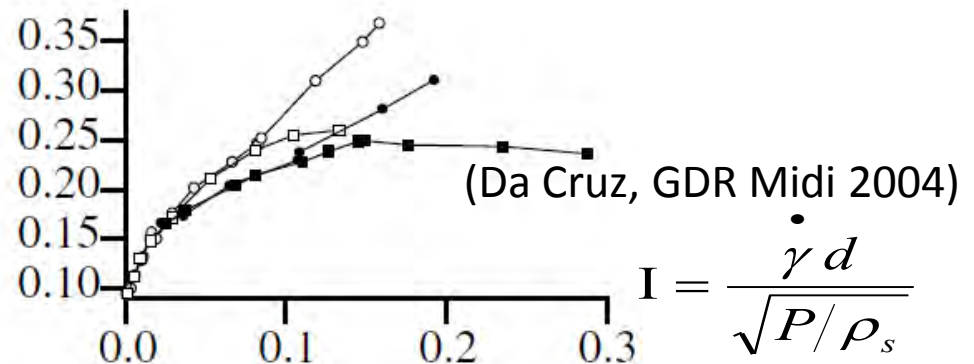
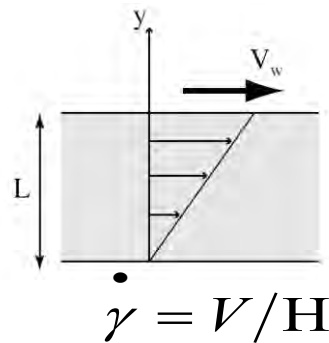
Internal (basal) μ from force balance at steady state



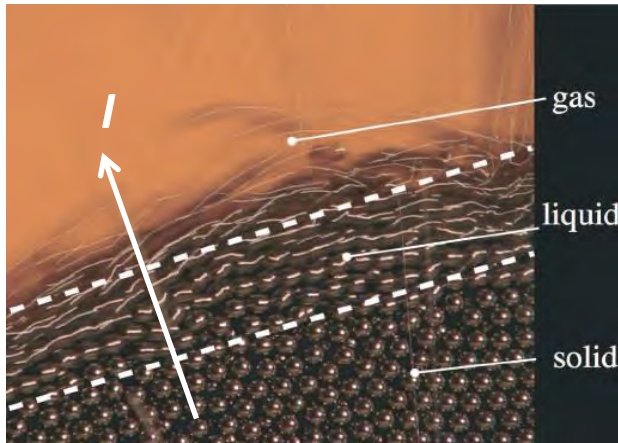
(Pouliquen 1999)

$$\frac{\|U\| d}{\sqrt{gh} h} = \alpha \frac{d}{h}$$

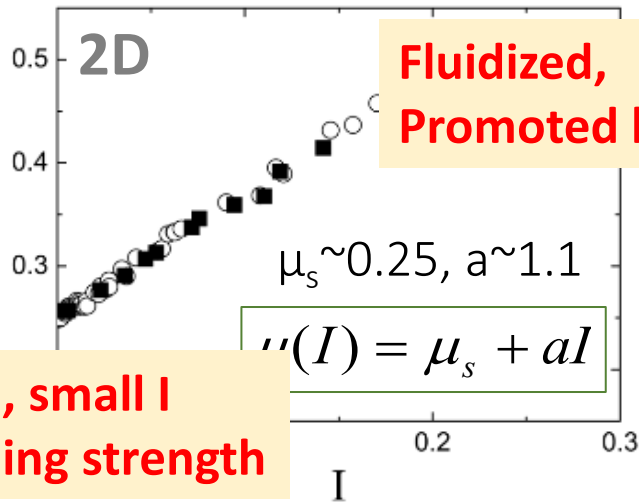
2D Confined flow DE simulation



Inertial number & $\mu(I)$ rheology law

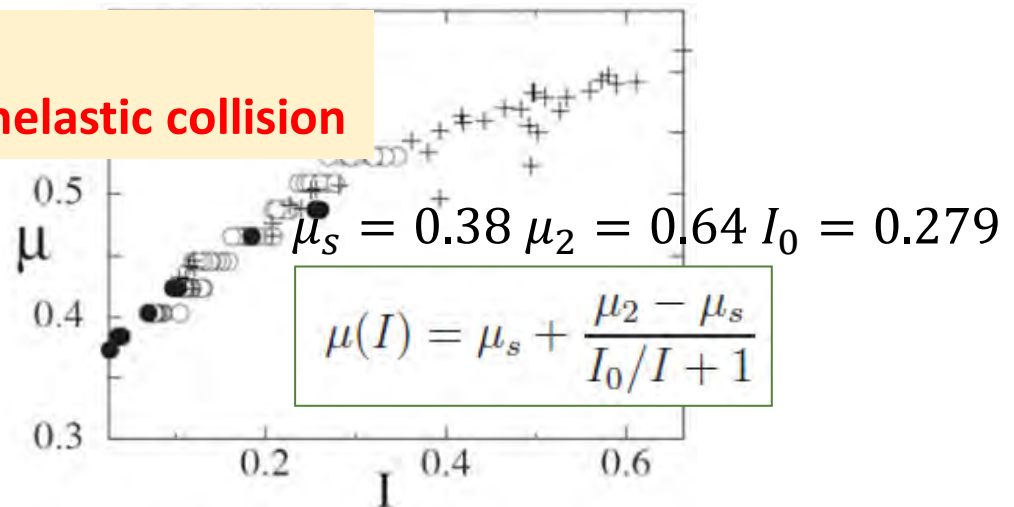


$$I = \frac{\dot{\gamma} d}{\sqrt{P/\rho_s}} \sim \frac{\text{Shear-induced streamwise motion}}{\text{transverse settling motion due to confinement}}$$



**Solid, small I
Yielding strength**

**Fluidized,
Promoted by inelastic collision**



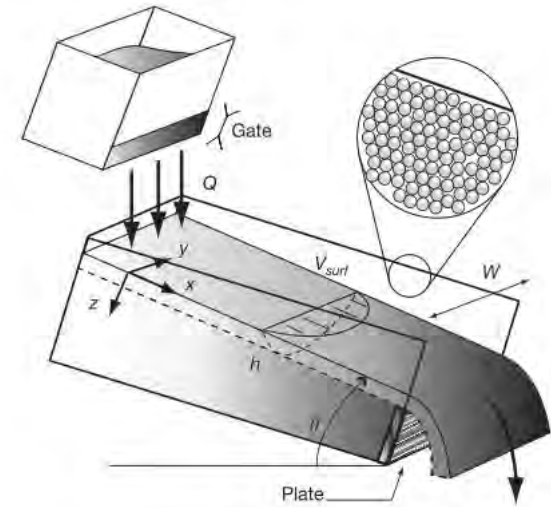
(Da Cruz 2004, GFR Midi 2004)

(Pouliquen 2006)

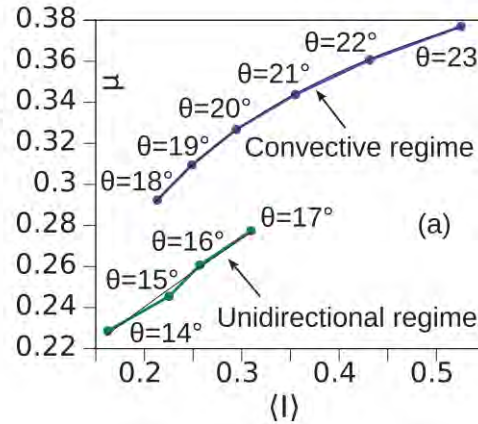
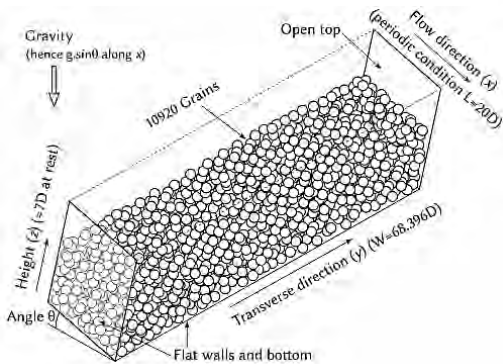
Remarks: boundary condition

Experiments are 3D: Lateral friction ?

- neglected when H/W is low
- included as Coulomb friction:
 $\text{hydro } P \times \text{constant } \mu_w$

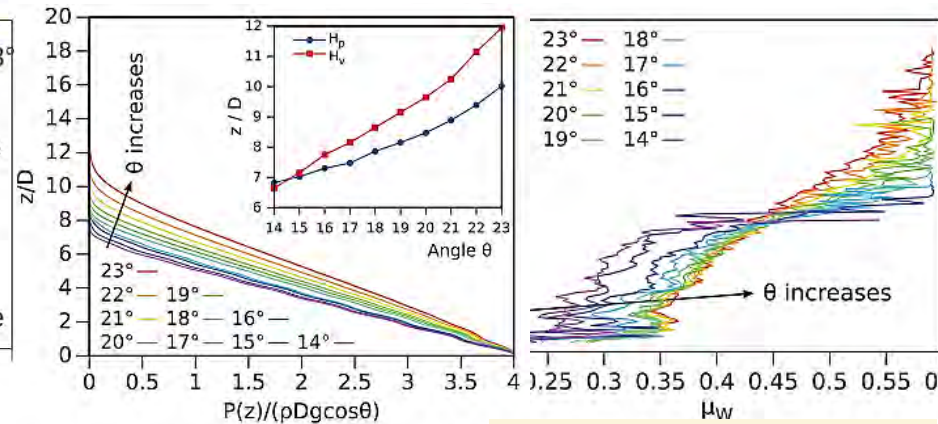


2D Numerical simulations → 3D



confirm internal μ -l

(Brodu, Richard, & Delannay 2013)

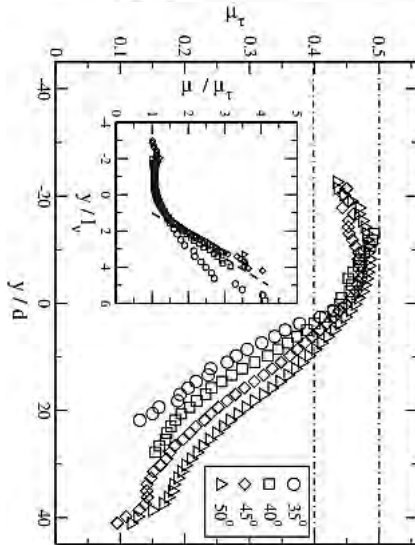
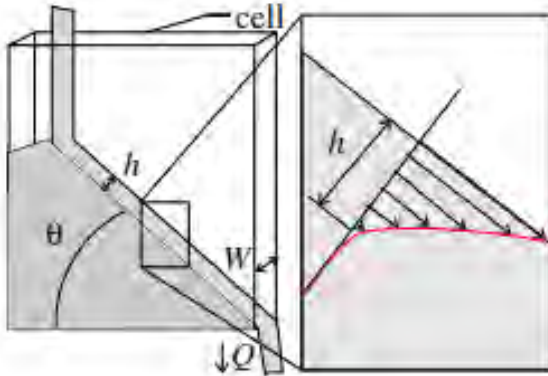


hydro P

Depth-weakening μ_w

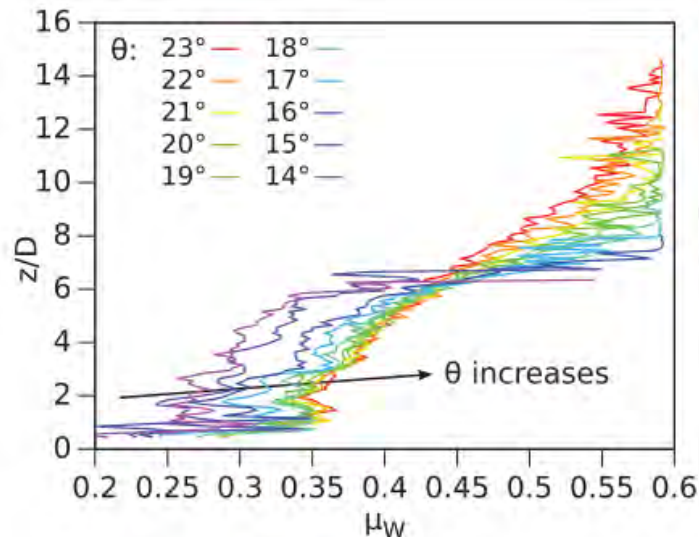
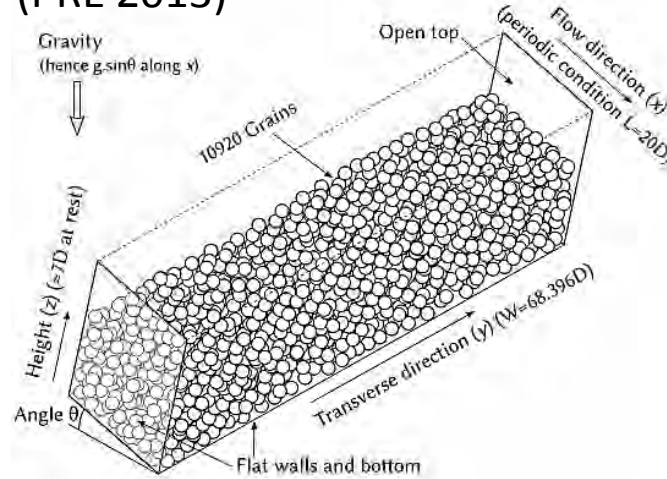
Non-constant wall friction coefficient (simulation based)

Richard et al. (PRL 2008)



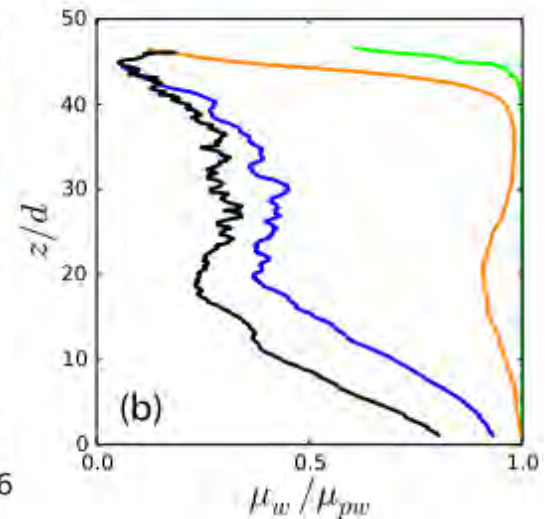
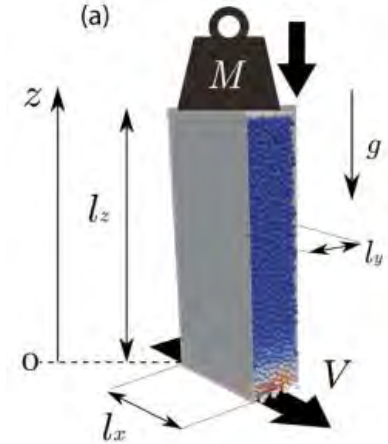
Tall, narrow

Brodu, Richard, Delannay
(PRE 2013)



Wide, shallow (loose)

Artoni & Richard (PRL 2015)



Tall, narrow (compact)

Questions:

Constitutive model: in unsteady/finite flows?

Boundary condition: experimental evidence?
Mechanism/model?

Internal μ **in unsteady non-uniform avalanche**

Inclined Flume Experiments

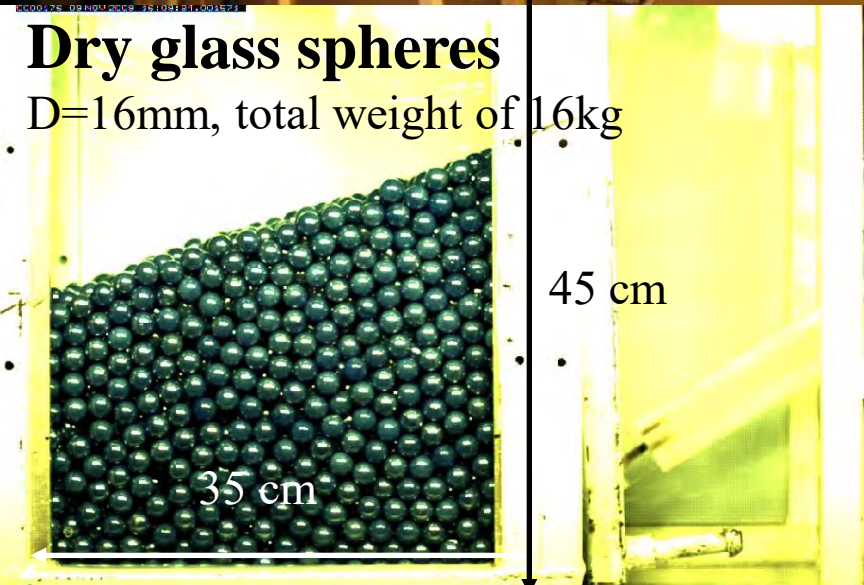
(indirect) image-based control-vol analysis

Laboratory Flume

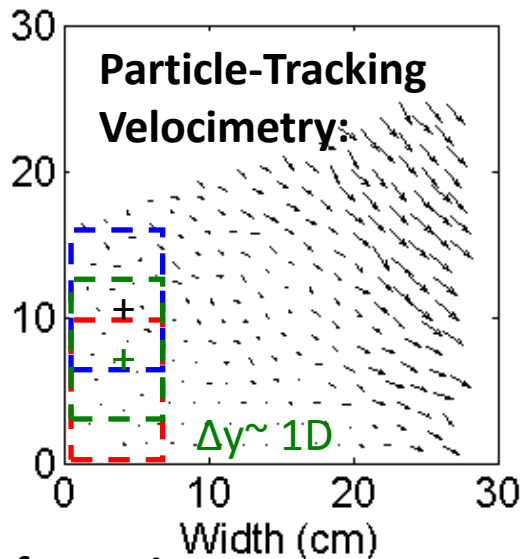
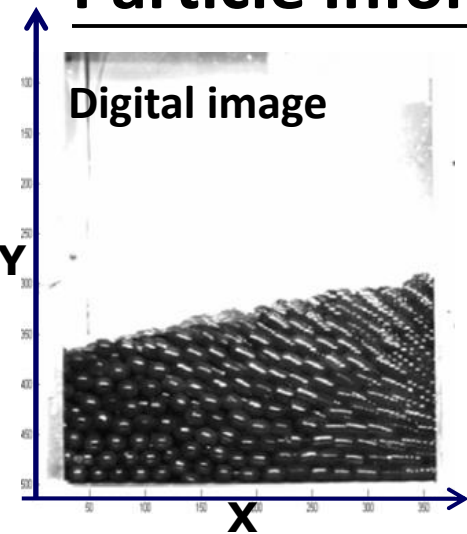
Camera : 500fps



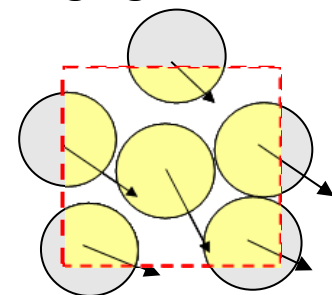
Reservoir



Particle Information

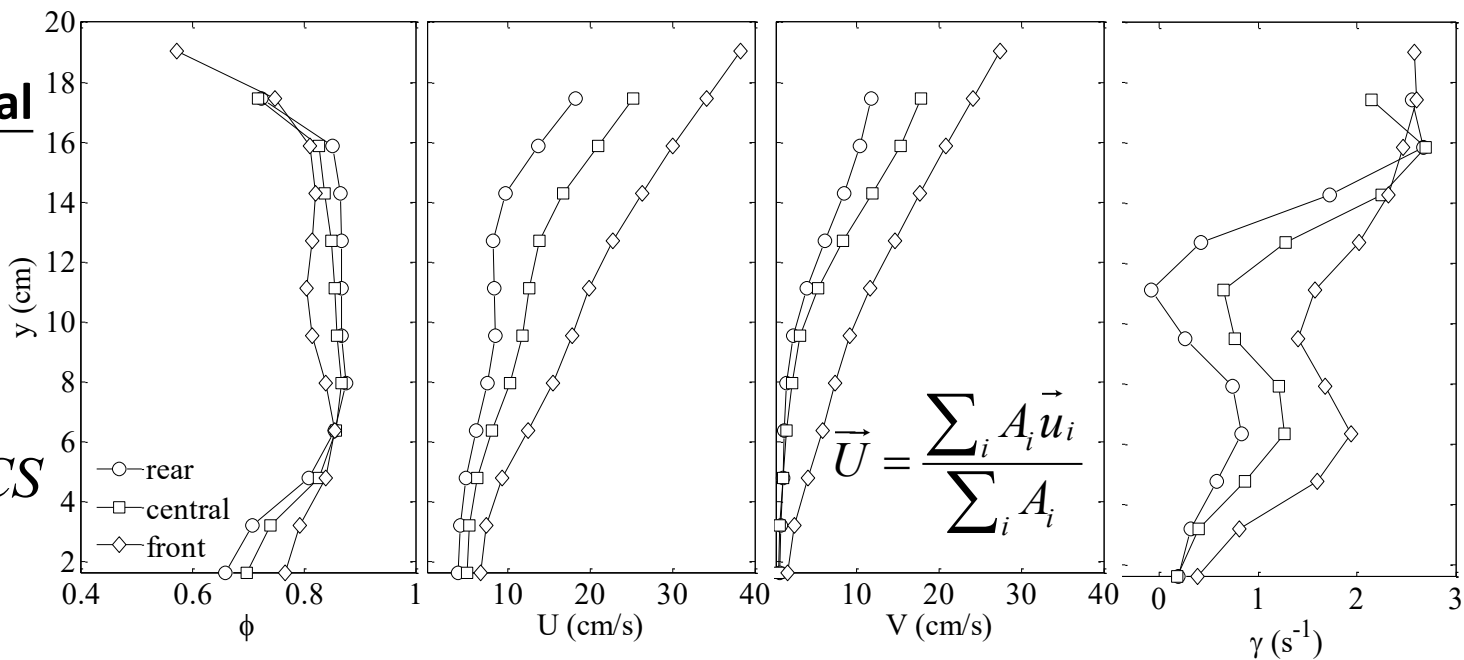


Area-weighted averaging

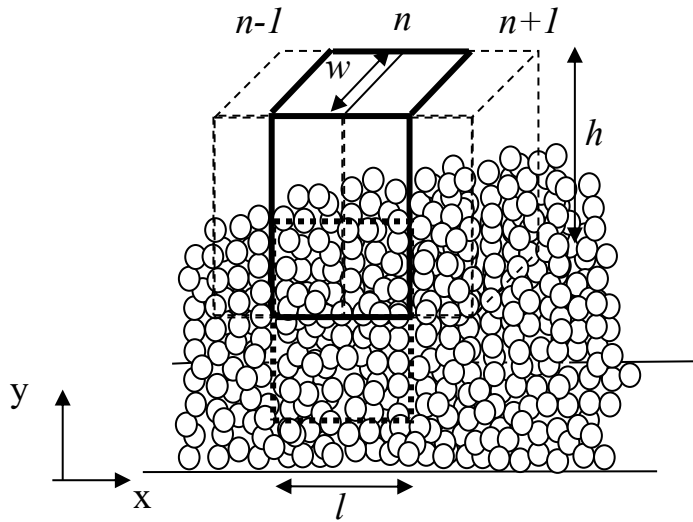


Instantaneous local bulk properties

$$\phi_n(x, y) = \sum A_i / CS$$

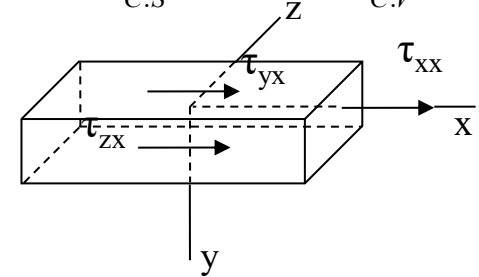


Quasi-2D Control Volume Analysis

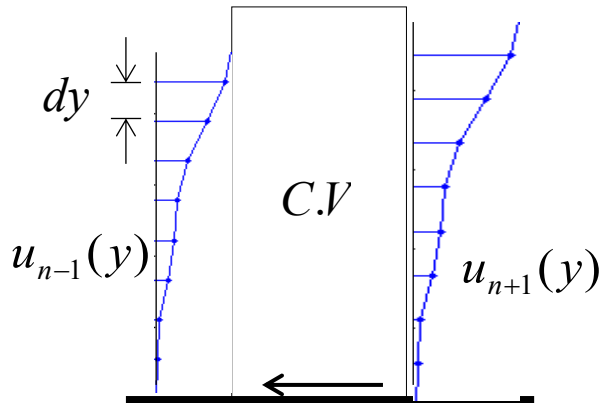


x-momentum conservation :

$$\iiint_{C.V} \frac{\partial}{\partial t} (\rho u_i) dV + \oiint_{C.S} \rho u_i u_j n_j dA_j = \oiint_{C.S} \tau_{ji} n_j dA_j + \iiint_{C.V} \rho f_i dV$$



$$\frac{\partial}{\partial t} w l \int_0^h \rho U dy + w \left[\int_0^h \rho U^2 dy \right]_{n-1}^{n+1} = -w g_y \left[\int_0^h \rho (h-y) dy \right]_{n-1}^{n+1} - 2F_w - F_B - w l g_y \int_0^h \rho dy$$



*Coulomb friction

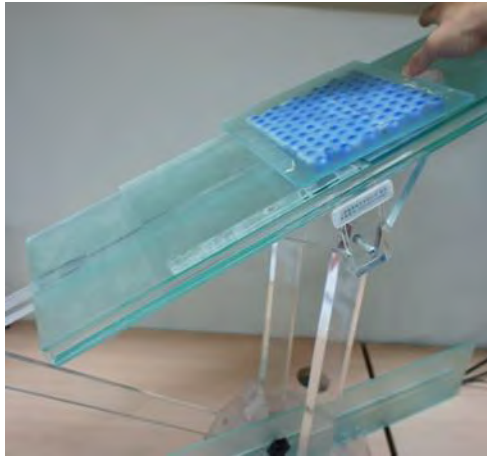
$$\int \tau_{zx} dA_z = \int \mu_w \tau_{zz} dA_z$$

*Hydrostatic normal stress, hence isotropic

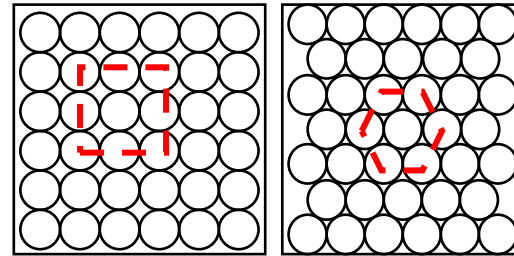
$$\tau_{zz} \approx \tau_{yy} \approx \tau_{zz} = \rho g_y h$$

Results

Sliding-table experiment using a layer of glued particles yields $\mu_w \sim 0.17$



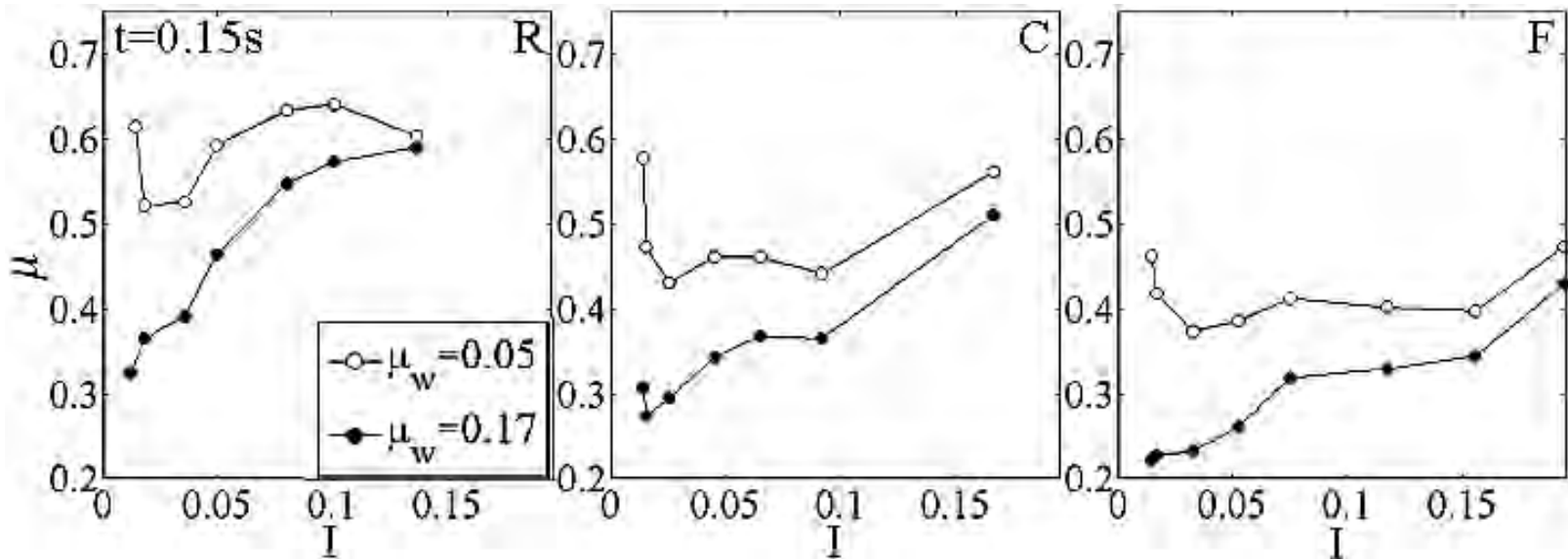
BCC
($\phi = 0.785$)

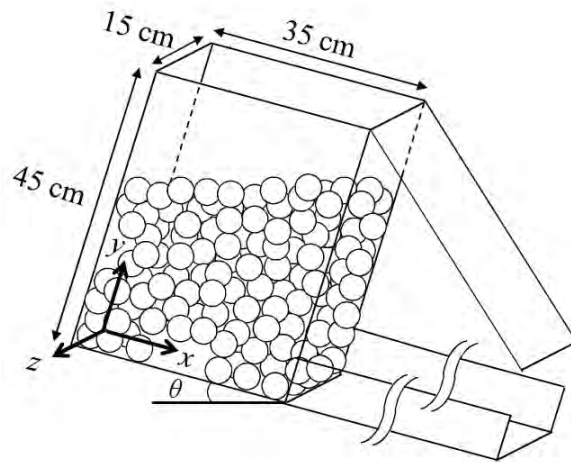


FCC
($\phi = 0.907$)

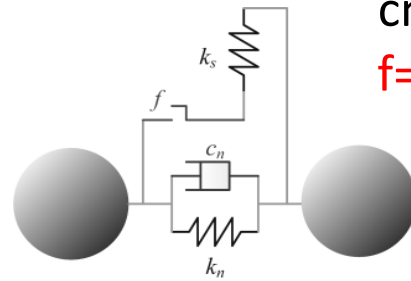
$$\alpha_{exp} = \alpha \phi_B + (1 - \alpha) \phi_F$$

$$\mu_w = \alpha \mu_{wB} + (1 - \alpha) \mu_{wF} \cong 0.171$$





$$\vec{F} = \vec{F}_n + \vec{F}_t$$



Classical soft-sphere contact model
 k_n , k_t (elasticity, Hertzian contact time)
 c_n (coefficient of restitution)
 $f=0.2$ by 'bulk' discharge flow rate

Internal μ in unsteady non-uniform avalanche

Validated Discrete element simulation *Yang et al. (PoF, 2013)*

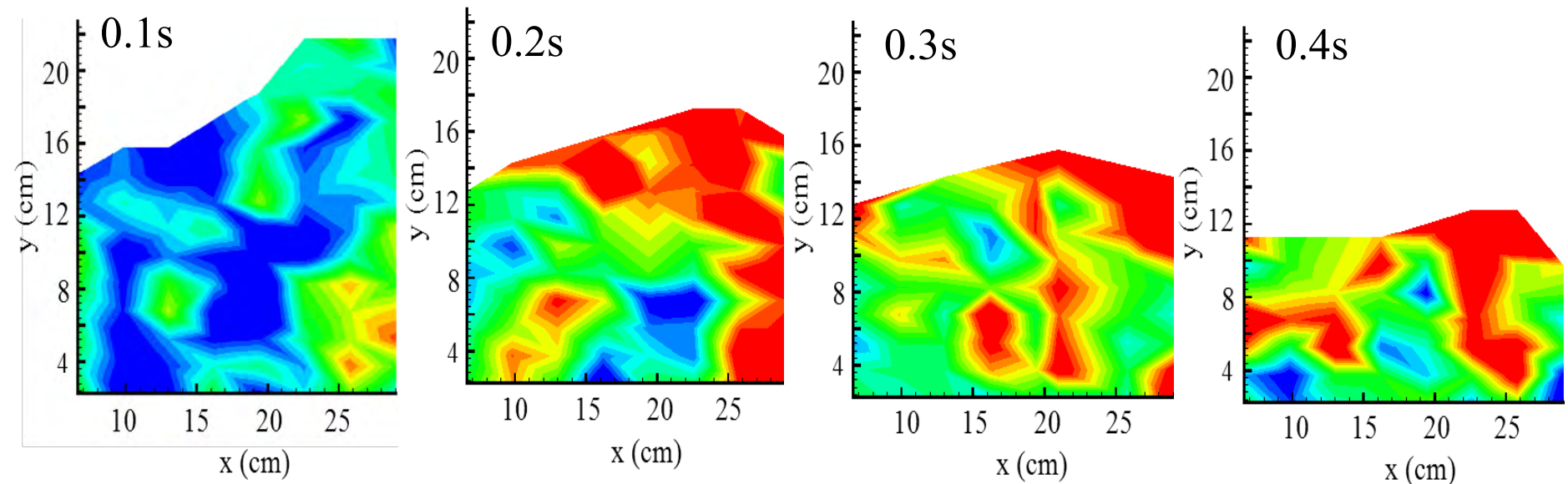
for direct force calculation

Virial Stress tensor for μ

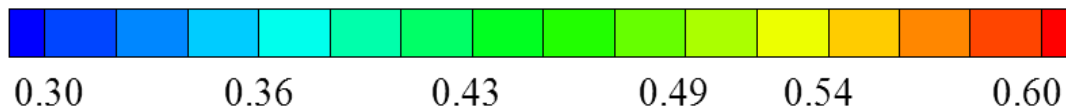
$$\sigma = \frac{1}{\Omega} \left[\frac{1}{2} \sum_{\substack{\alpha, \beta \in \Omega \\ \alpha \neq \beta}} \vec{F}^{\alpha\beta} \otimes \vec{r}^{\alpha\beta} - \sum_{\alpha} m^{\alpha} \delta v^{\alpha} \otimes \delta v^{\alpha} \right] \longrightarrow \mu = |\tau|/P$$

contact contribution kinetic contribution
(negligible for dense flow)

Second/first invariant
of stress tensor

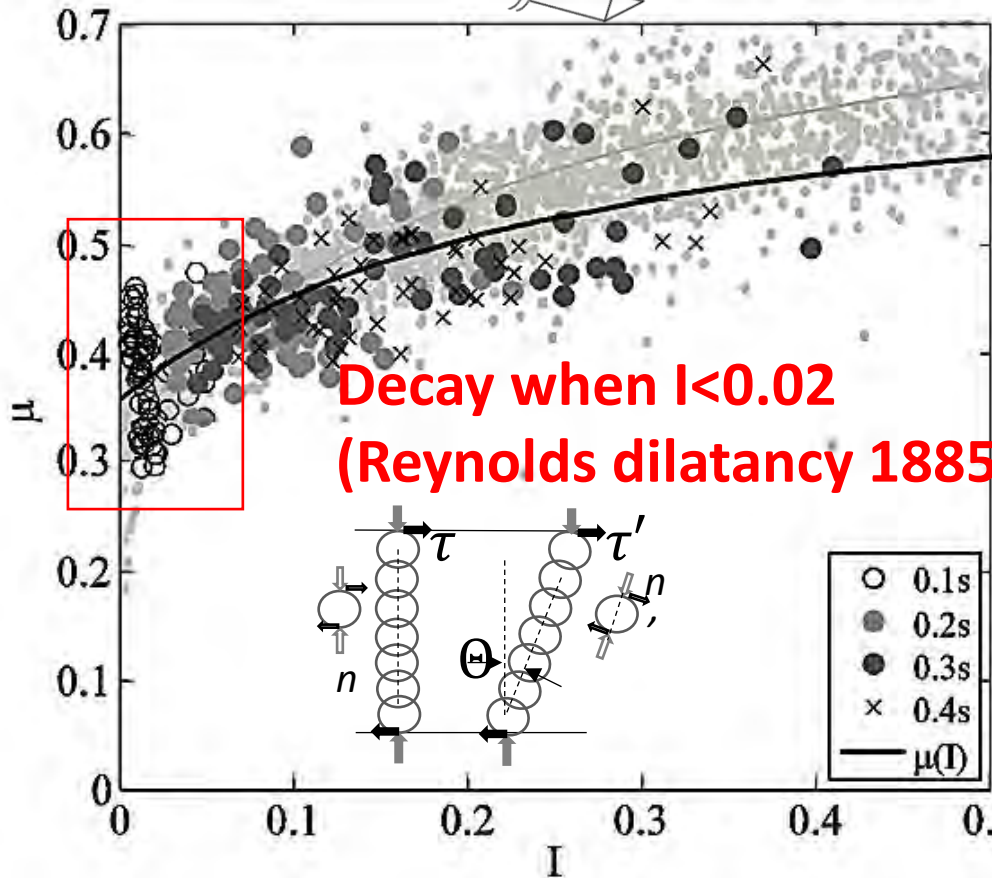
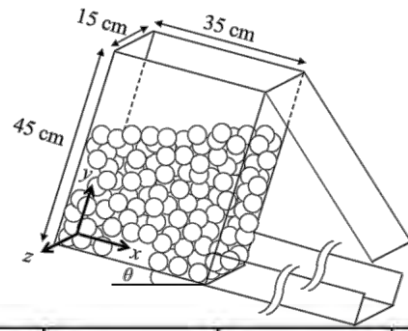


$\approx \tan 19^\circ$
(= 0.34)

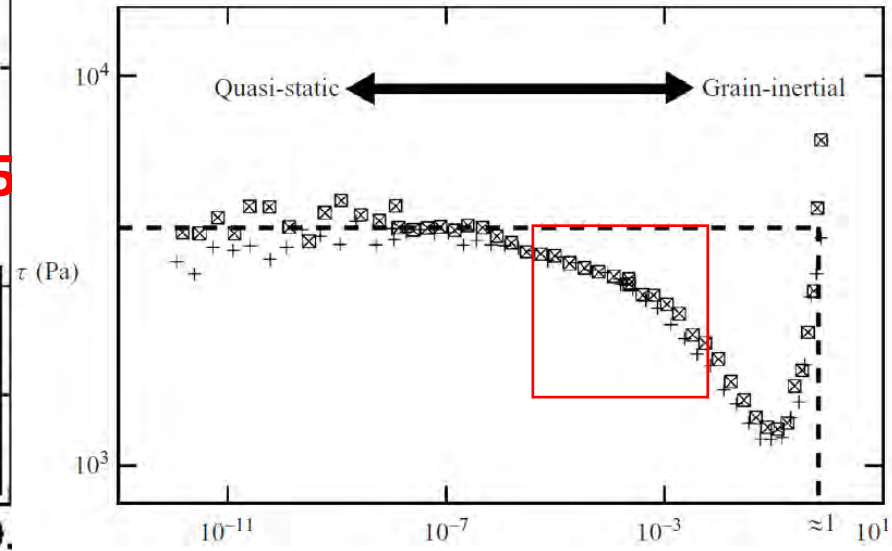
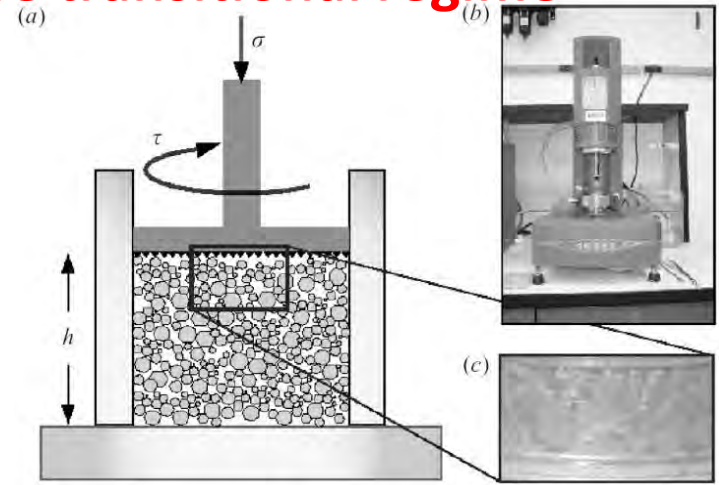


Yang & Huang (GM, 2016)

Instantaneous $\mu - I$ relation

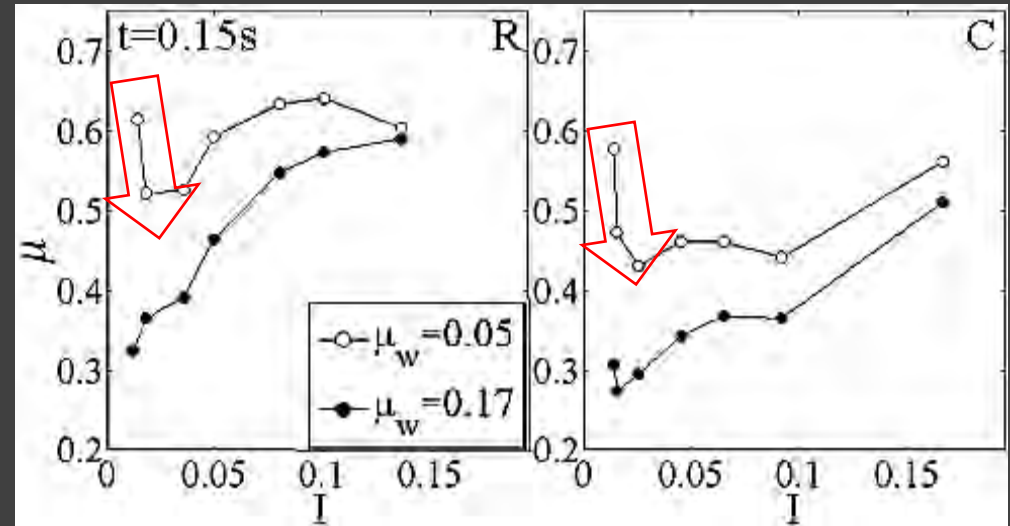
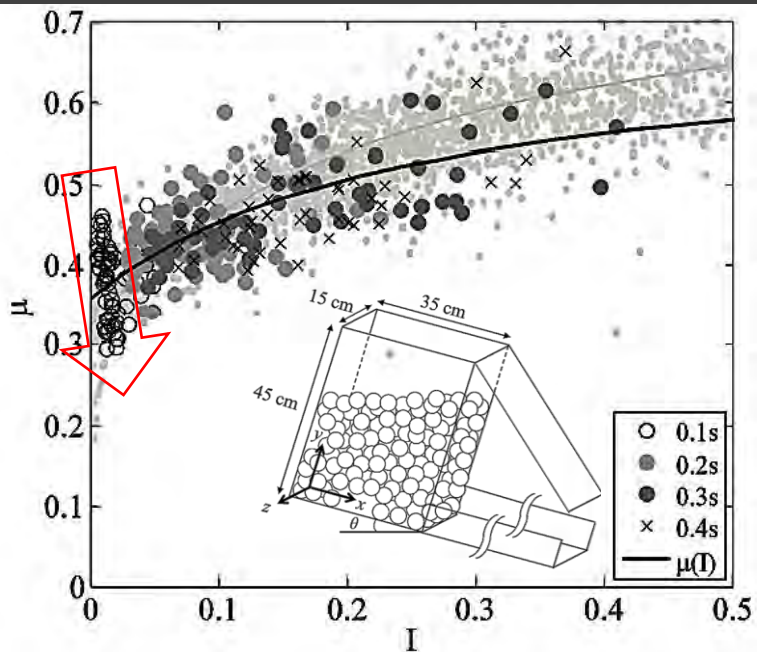


Measured shear-weakening at s-l phase transitional regime



Summary I

- Monotonically rising $\mu - I$ confirmed above $I_c \sim 0.02$



- Decay trend below I_c (with μ_w reduced from pure-sliding value)
- Transition as a bifurcation phenomenon

Boundary condition: μ_w

Direct measurement in steady uniform flows

Confirmation in real steady uniform flows

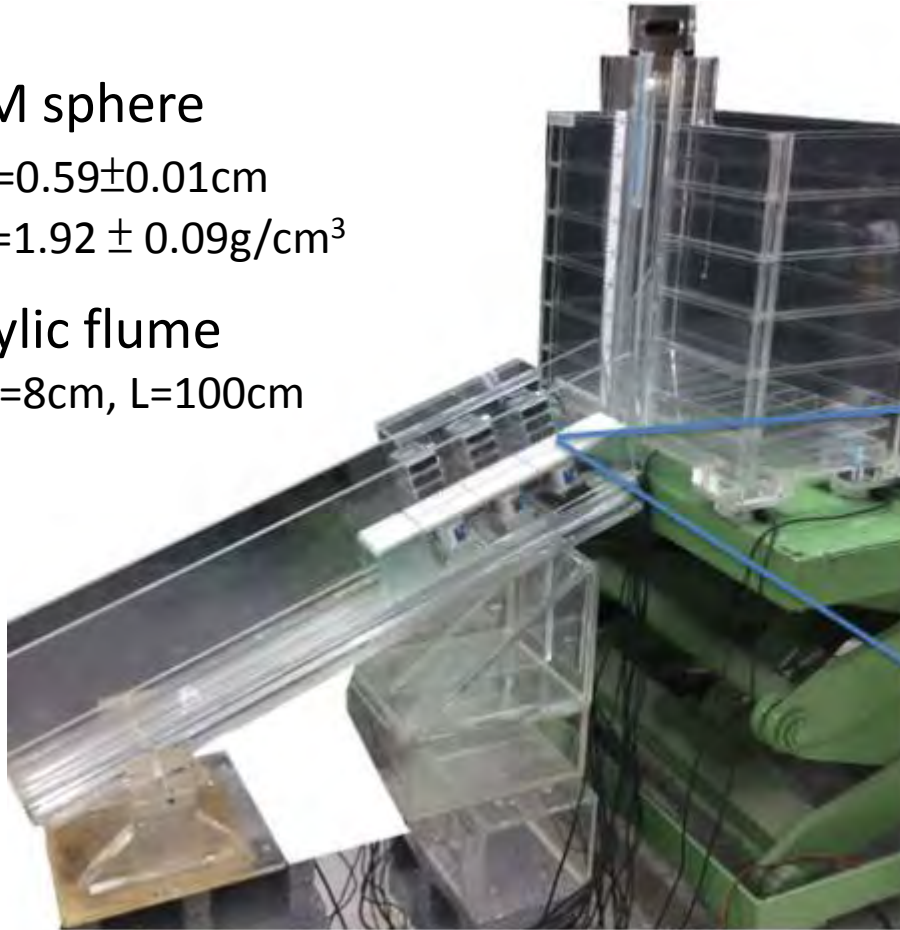
POM sphere

$$D=0.59\pm 0.01\text{cm}$$

$$\rho=1.92 \pm 0.09\text{g/cm}^3$$

Acrylic flume

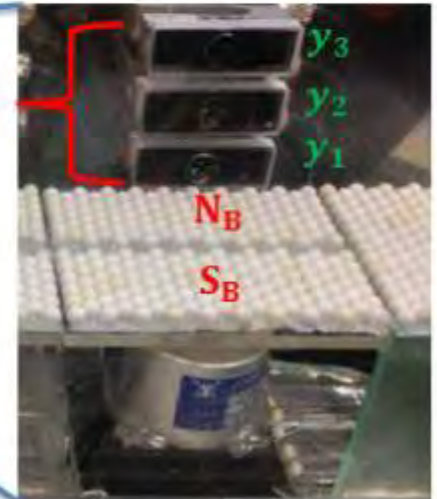
$$W=8\text{cm}, L=100\text{cm}$$



Direct force measurement
via load cell (LC) array

N or S in depth on side wall

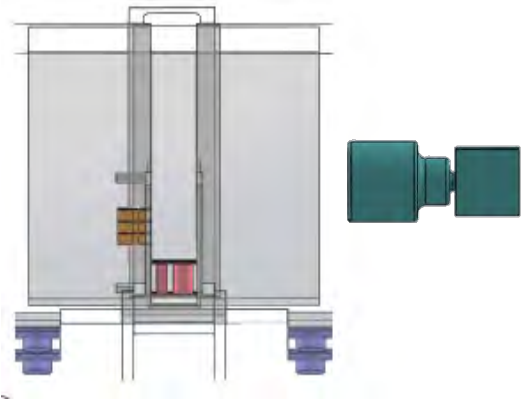
N_w or S_w



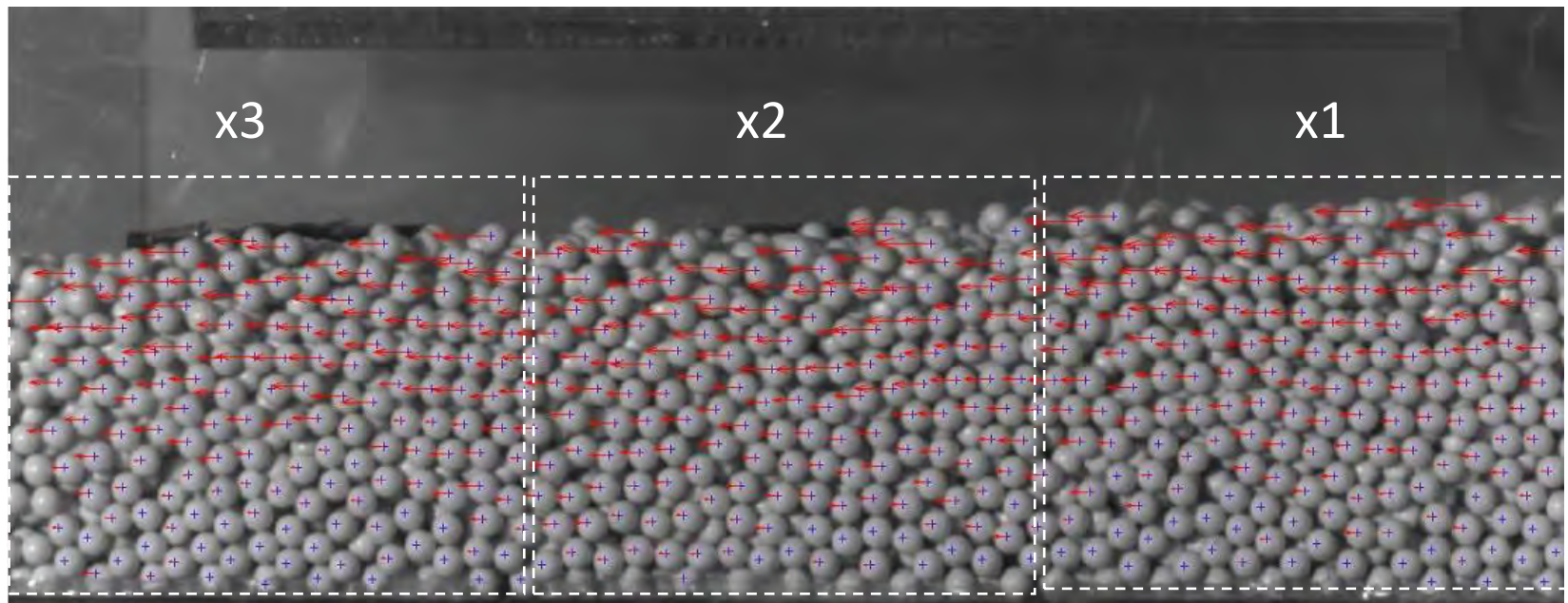
Concurrent N and S @ base

Roughened by spheres

Concurrent high-speed imaging

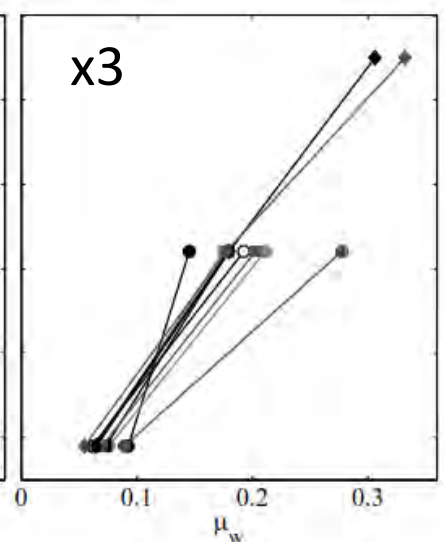
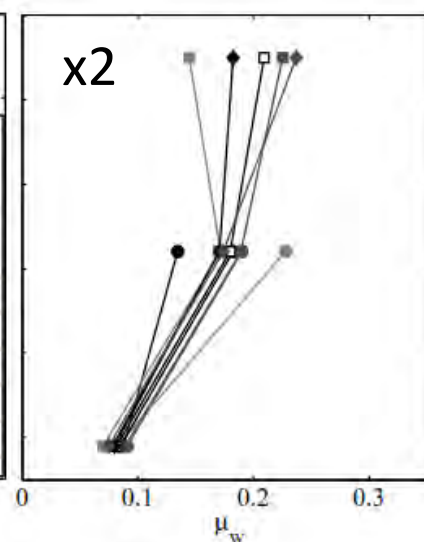
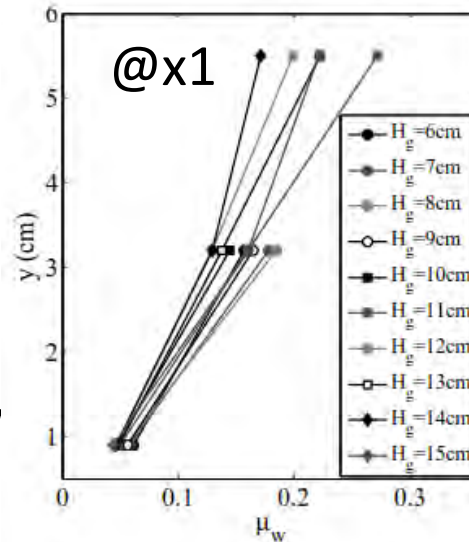
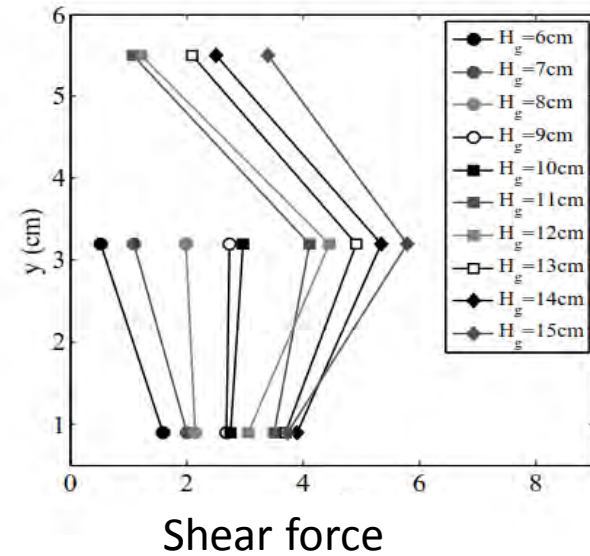
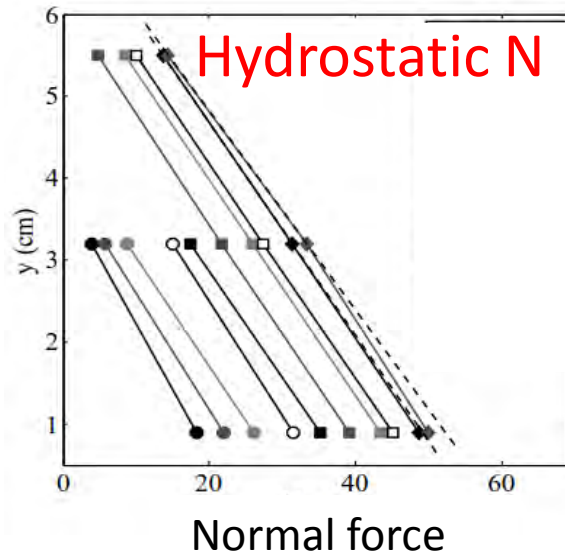


Indirect measurement [500pfs]
+ PTV (particle tracking velocimetry)
@ side: flow height $h(x)$
: solid volume fraction $\phi(x,y)$
: velocity $u(x,y)$



Wall μ_w

Steady mean
LC data



$$\mu_w = S_w / N_w$$

Non-constant
Decays in depth
Grows downstream

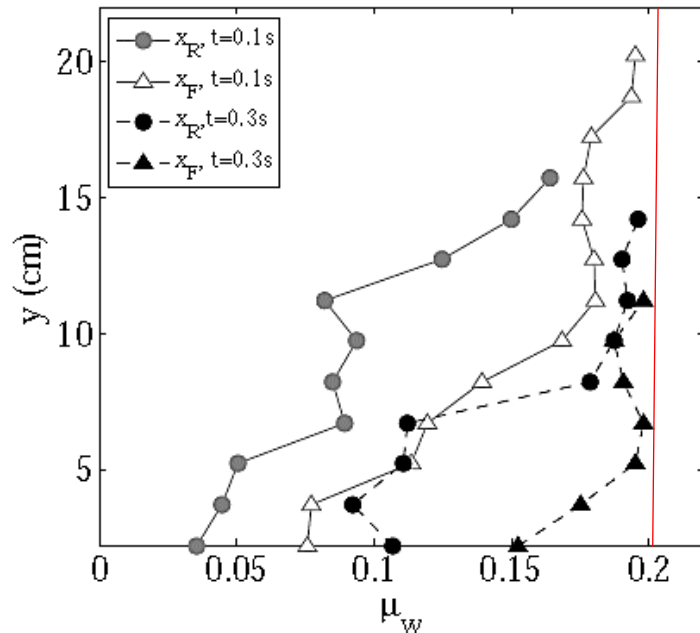
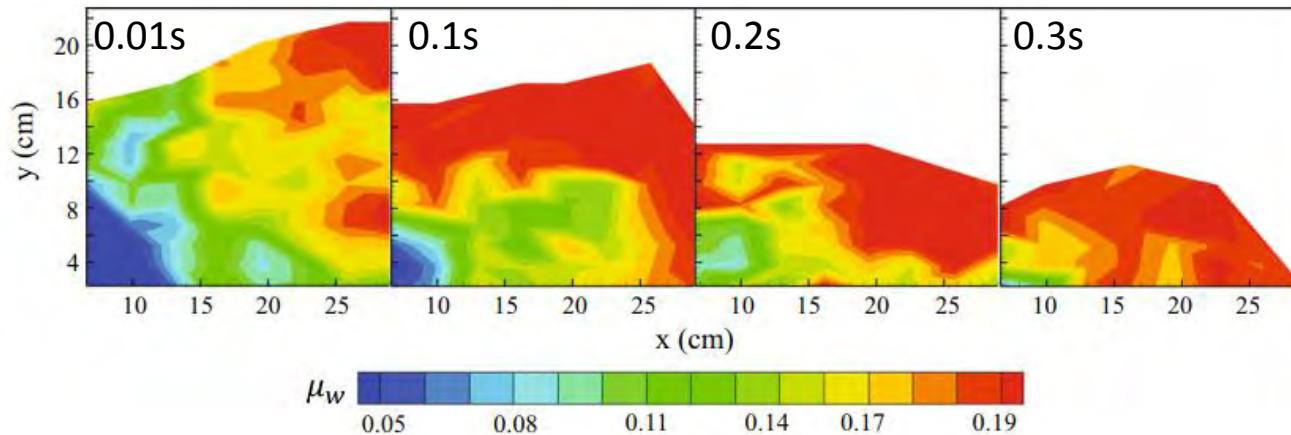
Boundary condition: μ_w

DEM simulated avalanche

DEM-rendered μ_w

$$\sigma_w = \sum_{\alpha \in A} \vec{F}^{\alpha w} / \Lambda$$

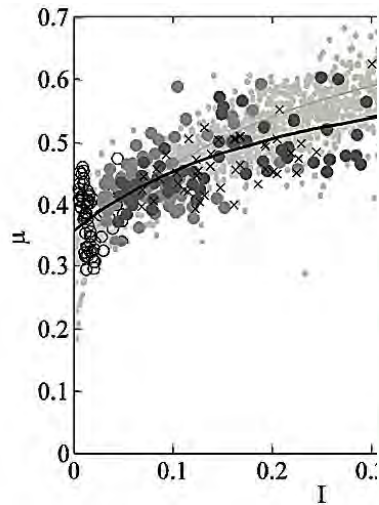
Bulk friction coefficient is non-constant: depth-weakening & flow-dependent
Always smaller than the microscopic sphere-wall $f=0.2$



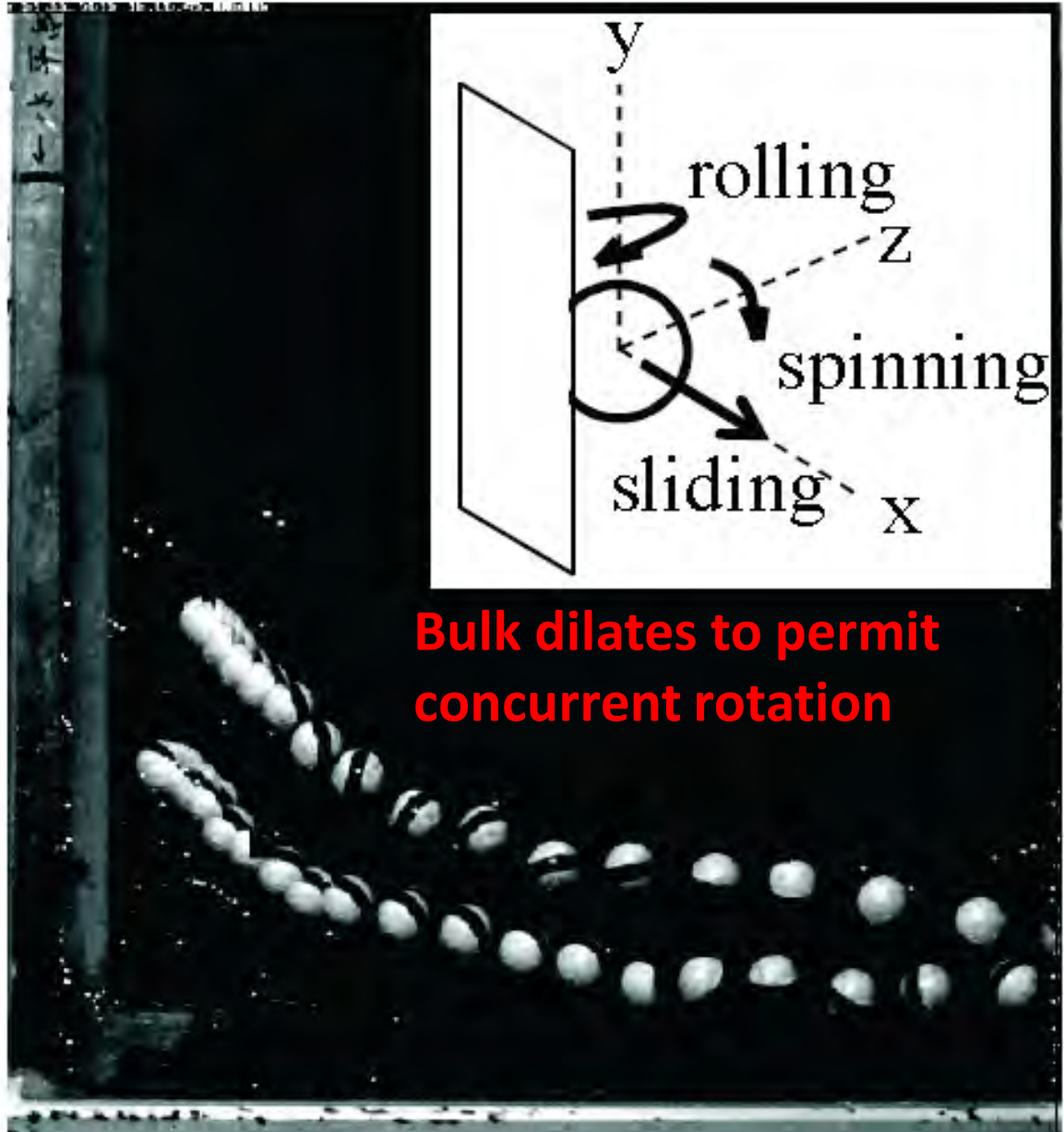
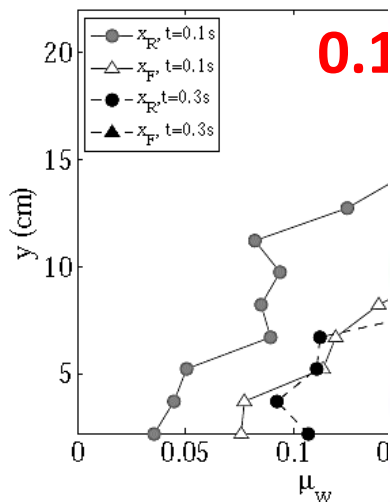
**Depth-decaying
Growing towards
'microscopic' f**

Inference of reduced μ_w

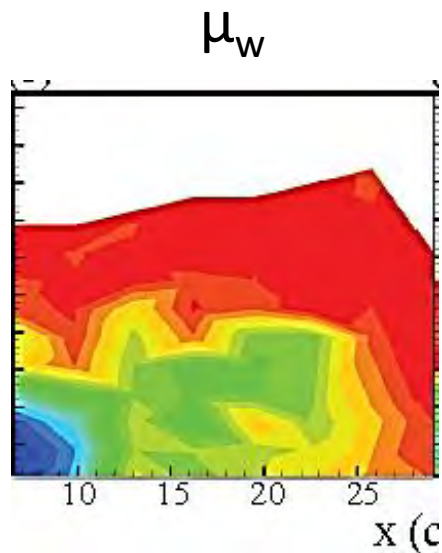
1. Decay of internal μ is physical



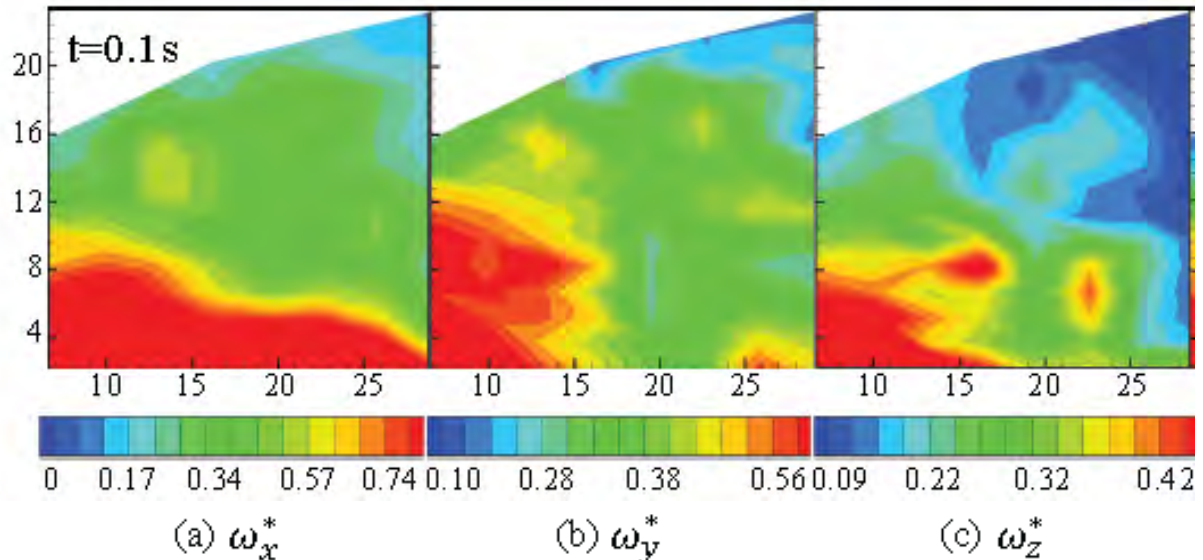
2. Simulated μ_w lower than sliding



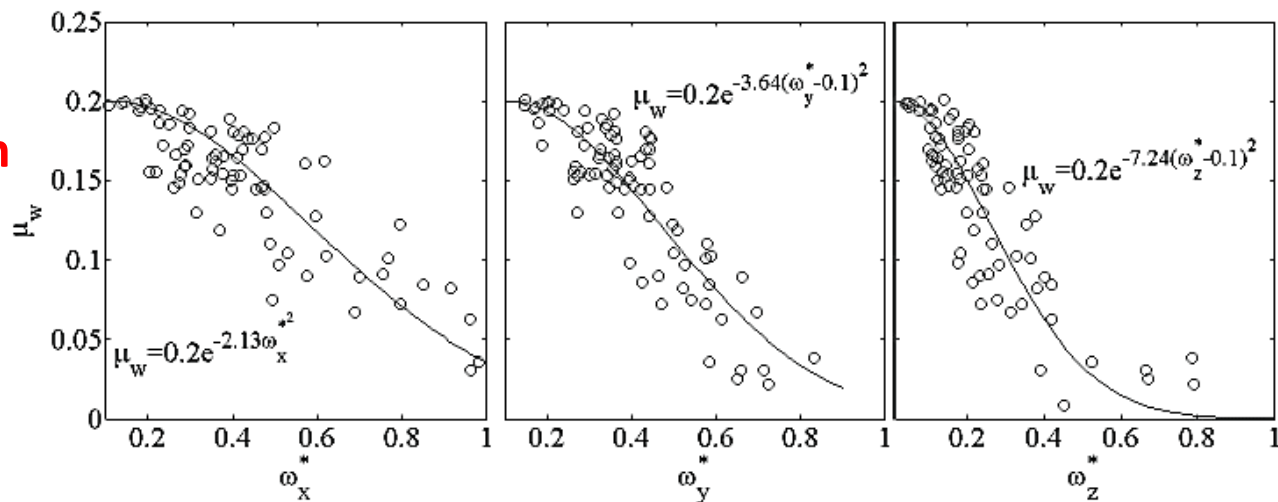
Rotation as a weakening mechanism



Normalized angular speeds

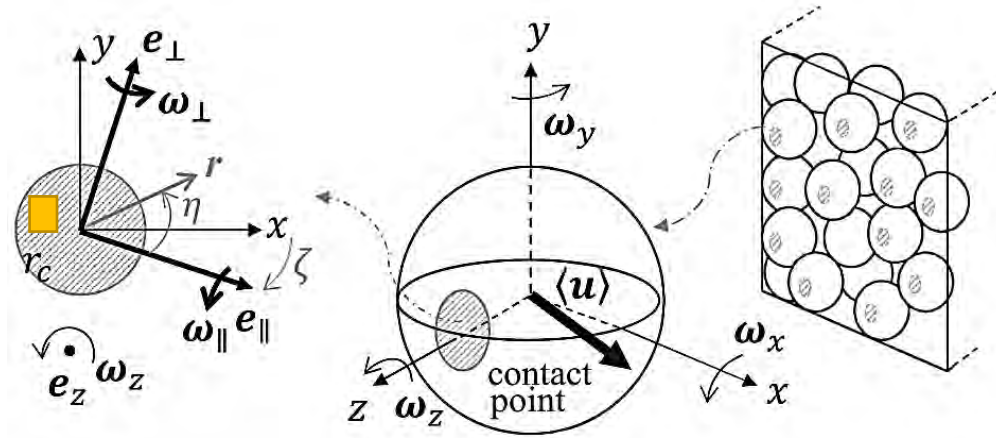
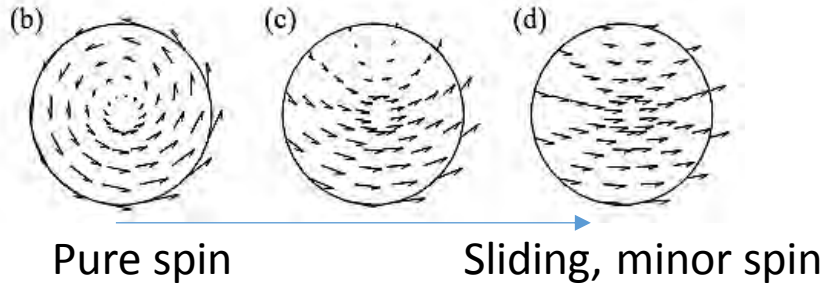


Strong correlation between μ_w & scaled angular speeds



Microscopic interaction model

Farkas et al. (PRL 2002)



Coulomb friction is 'more' valid over dA along \mathbf{u}_{tot} modified by grain rotation

$$\mathbf{F} = -\frac{f^{sw} P}{A_c} \int \mathbf{u}_{tot} / |\mathbf{u}_{tot}| dA$$

$$\begin{aligned} \tilde{\mathbf{u}}_{tot} = & (\tilde{u}_\parallel + R\tilde{\omega}_\perp - r \sin \eta \tilde{\omega}_z) \mathbf{e}_\parallel + (-R\tilde{\omega}_\parallel + r \cos \eta \tilde{\omega}_z) \mathbf{e}_\perp \\ & + (\tilde{u}_z + r \sin \eta \tilde{\omega}_\parallel - r \cos \eta \tilde{\omega}_\perp) \mathbf{e}_z \end{aligned}$$

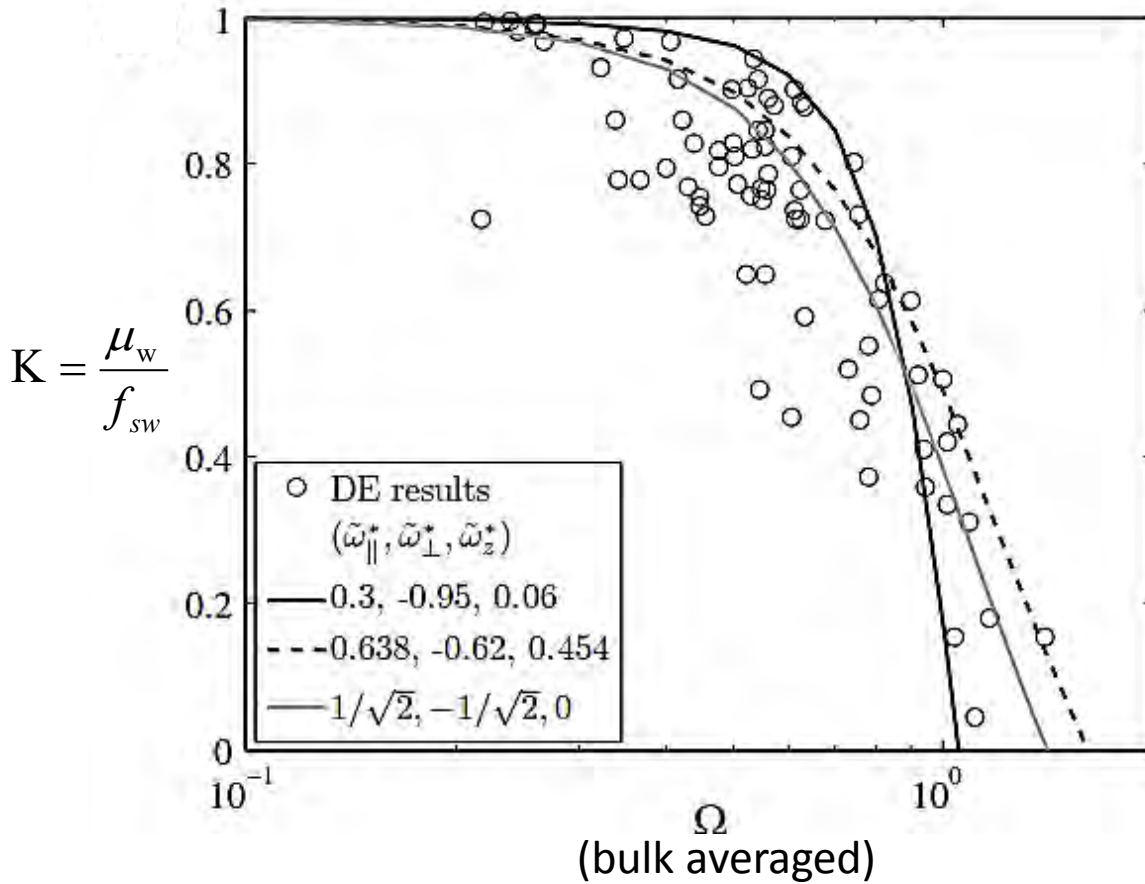
$$\mu_w = f^{sw} K(\Omega, \tilde{\omega}^*),$$

Rotation index

$$K(\Omega, \tilde{\omega}^*) = (\pi r_c^{*2})^{-1} \int_0^{2\pi} \int_0^{r_c^*} \frac{\tilde{\mathbf{u}}_{2D} \cdot \mathbf{e}_\parallel}{|\tilde{\mathbf{u}}_{2D}|} r^* dr^* d\eta$$

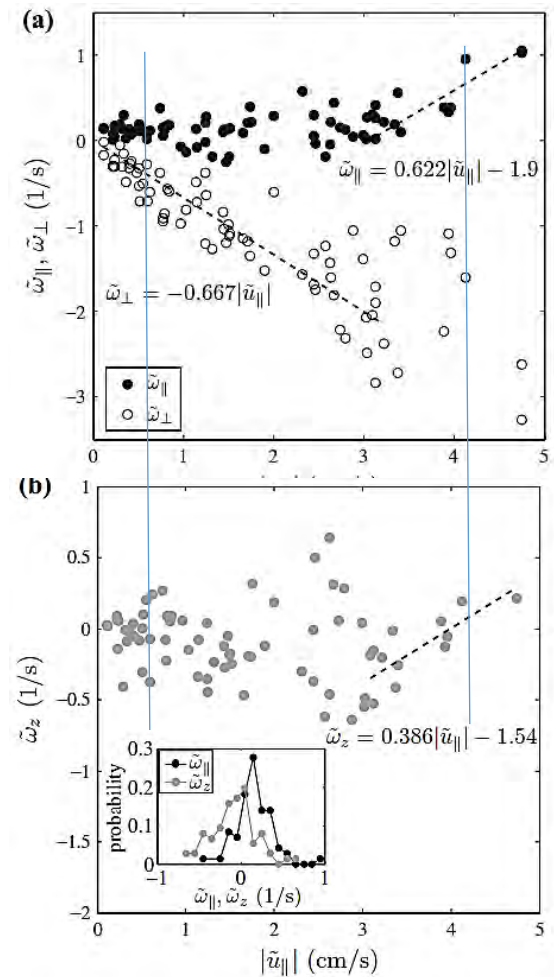
$$\Omega = \frac{R|\omega|}{|u_\parallel|}$$

Numerical evidence



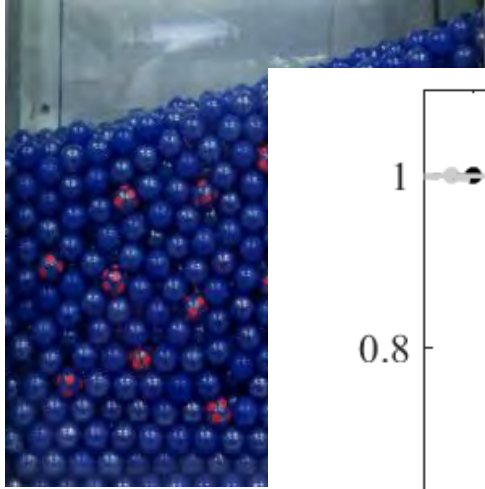
$$K(\Omega, \tilde{\omega}^*) = (\pi r_c^{*2})^{-1} \int_0^{2\pi} \int_0^{r_c^*} \frac{\tilde{\mathbf{u}}_{2D} \cdot \mathbf{e}_{\parallel}}{|\tilde{\mathbf{u}}_{2D}|} r^* dr^* d\eta$$

$$K_o(\Omega, \tilde{\omega}_{\parallel}^*, \tilde{\omega}_{\perp}^*) = \frac{1 + \Omega \tilde{\omega}_{\perp}^*}{[(1 + \Omega \tilde{\omega}_{\perp}^*)^2 + (\Omega \tilde{\omega}_{\parallel}^*)^2]^{1/2}}$$



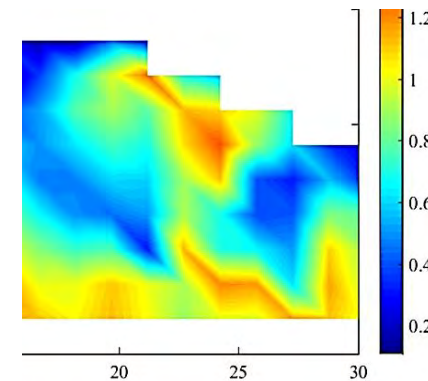
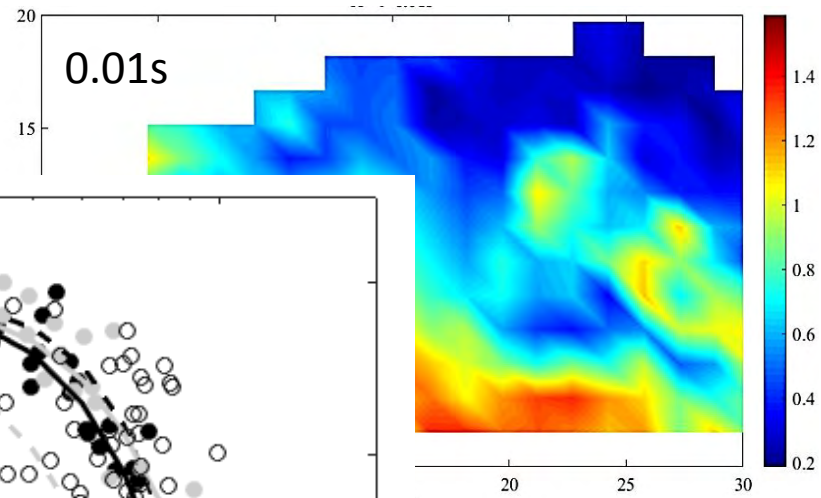
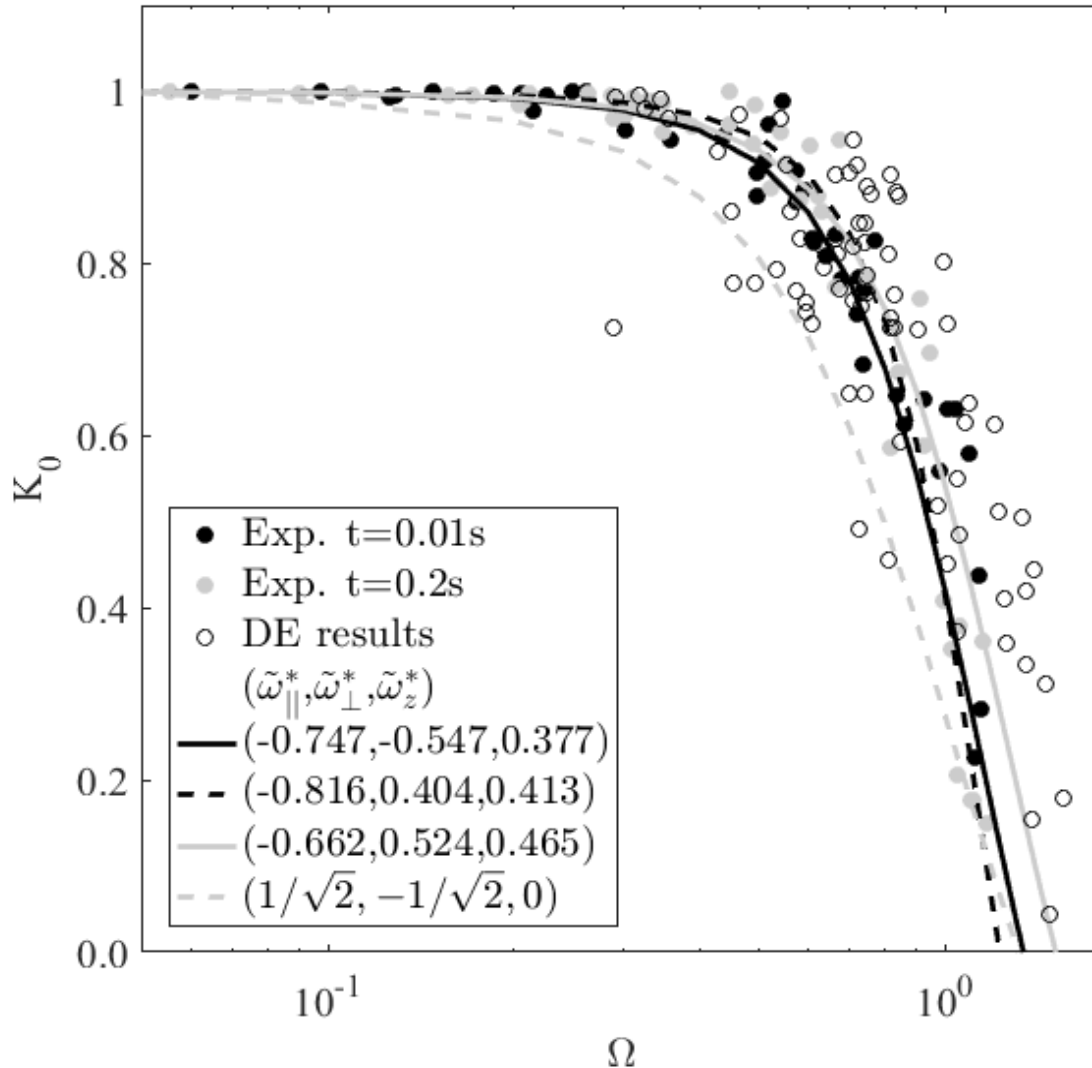
Explicit approximation

Experimental evidence for Ω



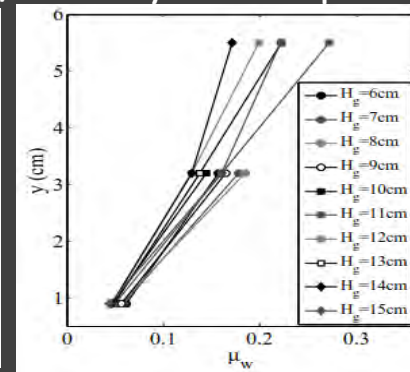
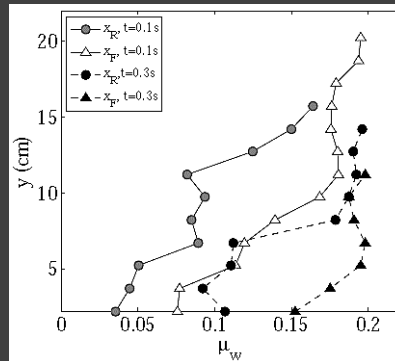
Markers to m
Bright spots t

Contour of sp



Summary II

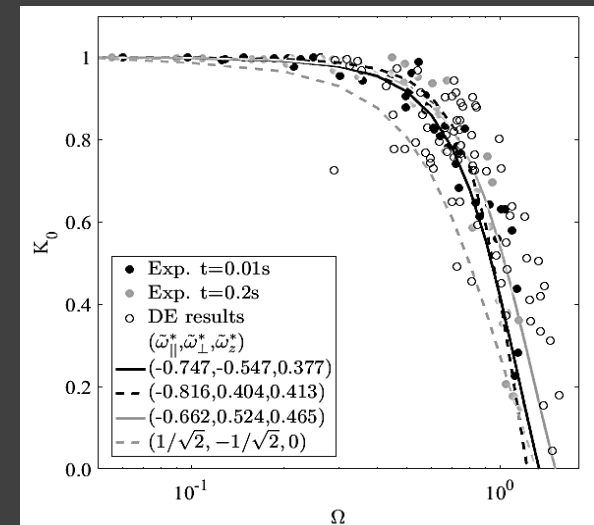
- Coulomb lateral wall friction requires a **non-constant developing μ_w**
 Depth-weakening simulated avalanche / steady flow experiments



- Reveal concurrent **rotation as the friction reduction mechanism**
 Degradation function $K(\Omega)$ from grain-grain f

$$K_o(\Omega, \tilde{\omega}_{\parallel}^*, \tilde{\omega}_{\perp}^*) = \frac{1 + \Omega \tilde{\omega}_{\perp}^*}{[(1 + \Omega \tilde{\omega}_{\perp}^*)^2 + (\Omega \tilde{\omega}_{\parallel}^*)^2]^{1/2}}$$

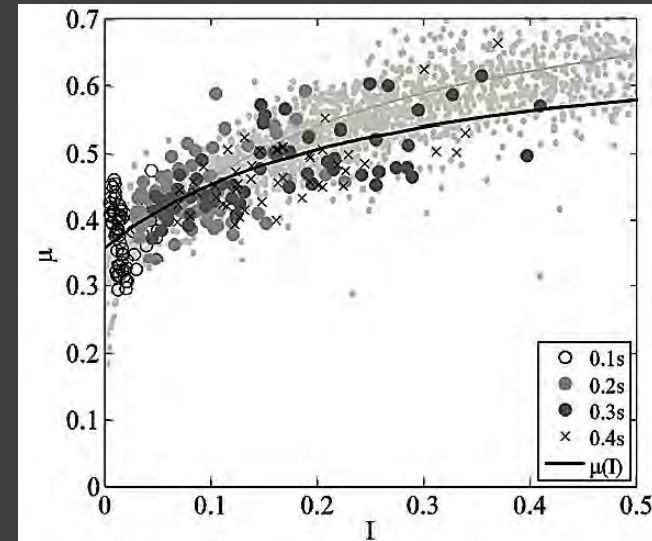
simulation / experiment



Conclusion

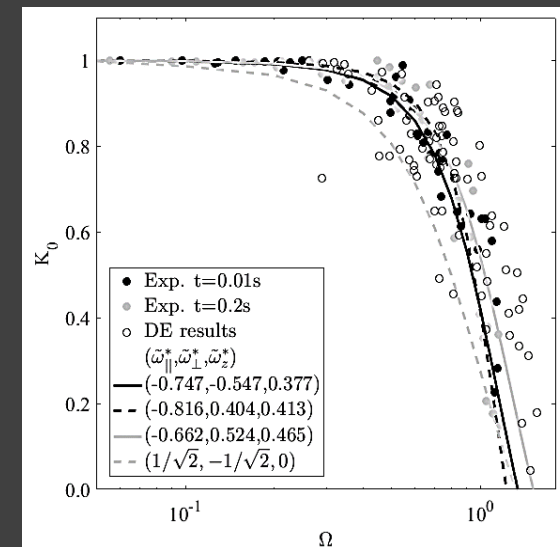
Bulk internal friction coefficient

- Monotonic rise of $\mu - I$ above $I_c \sim 0.02$
- **Decay trend below I_c**
- Non-monotonicity across I_c as a phase transition / bifurcation



Coulomb wall friction coefficient

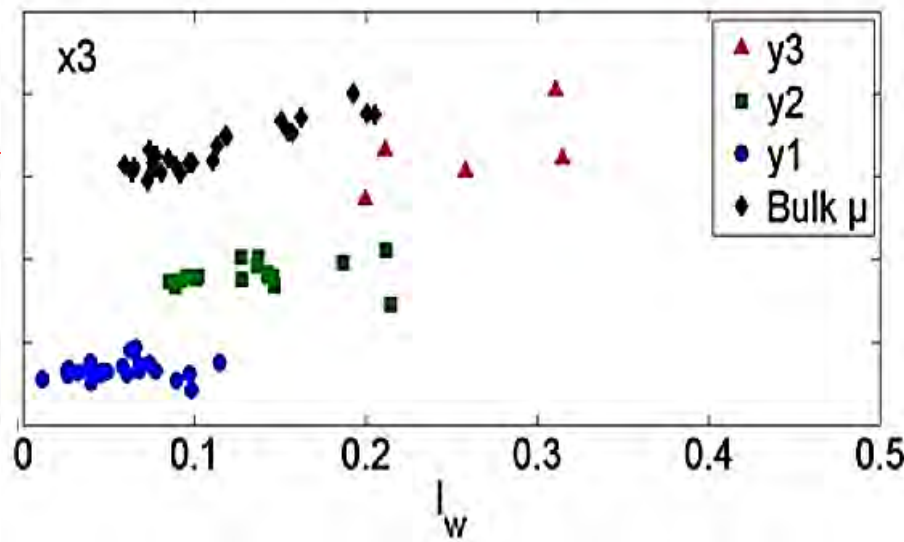
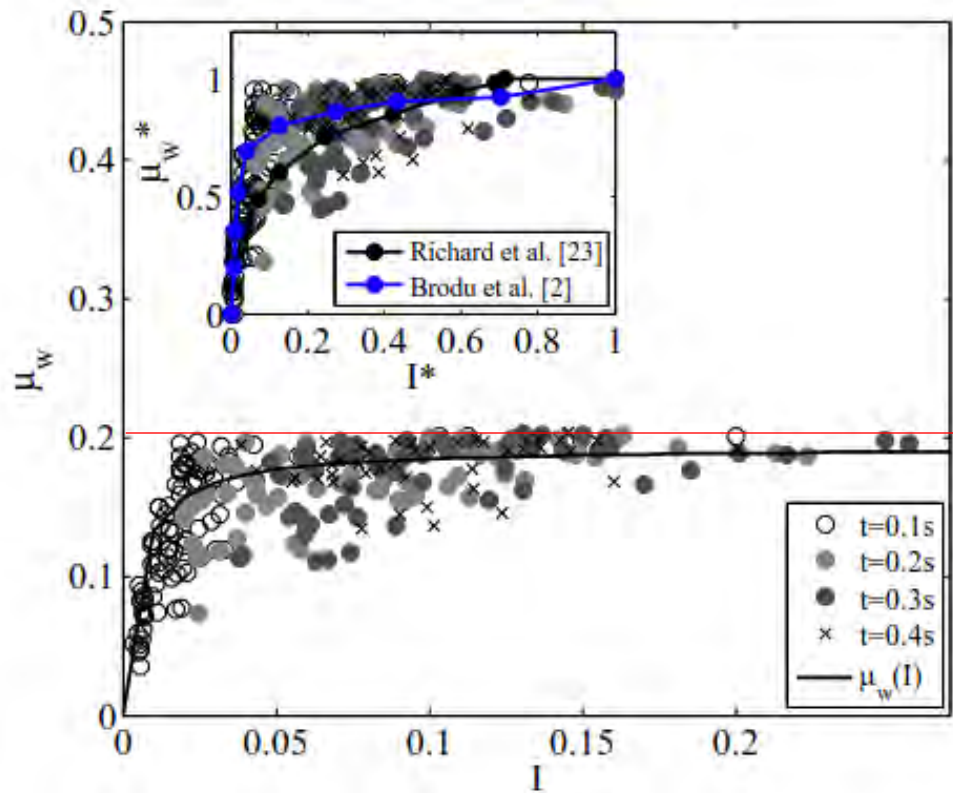
- **Non-constant μ_w**
Depth-weakening, developing
- Grain **rotation to friction degradation**
- Degradation function $K(\Omega)$ from micro f





Thank You

Credits to 黃永達、林正釧、邱廷彥、李庚霖



μ_w much smaller than μ

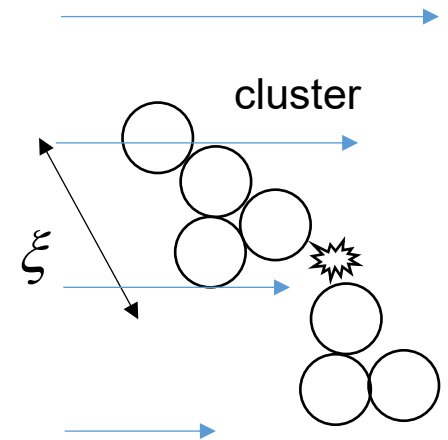
Flow dynamics away from jamming

- Small non-local effect ($l^2 \nabla^2 I \ll 1$)
- By Taylor expansion and scaling arguments, we have $\beta=2$ and an eddy-viscosity-like stress scaling

$$\tau \sim \rho \xi^2 \dot{\gamma}^2$$

- Correlation length $\xi(\mu) = Ad [r(\mu) - r_c]^{-1/2}$
- Long-range momentum transmission due to collisions between clusters.

Ertas & Halsey 2002; Pouliquen 2004; Staron 2008;
Mills et al 2013

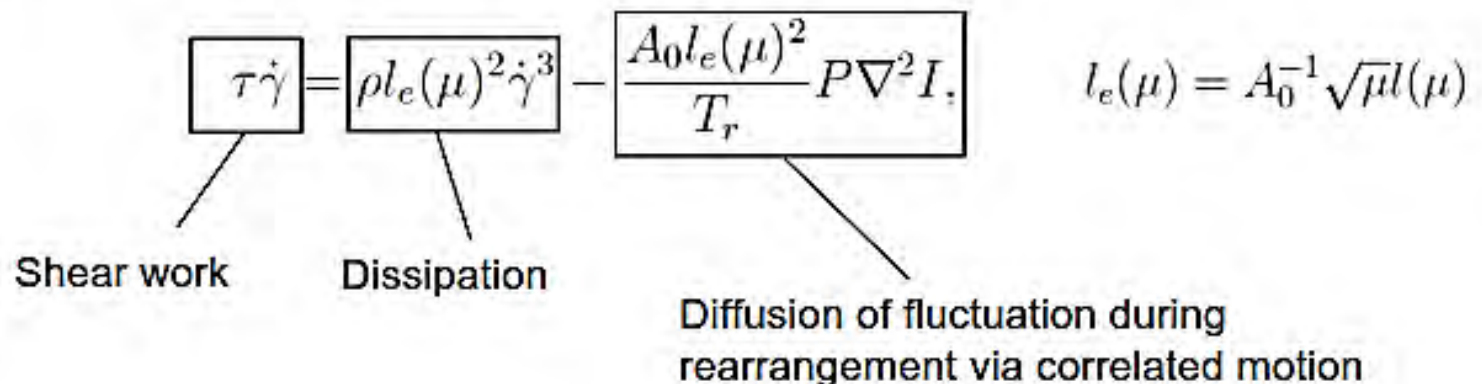


Bistability-free approximation

- In the limit of $\chi=0$

$$t_0 \frac{DI}{Dt} = \zeta^2 \nabla^2 I + [r(\mu) - r_c] I - BI^3,$$

- Single threshold μ_{stop}
- Steady-state energy balance



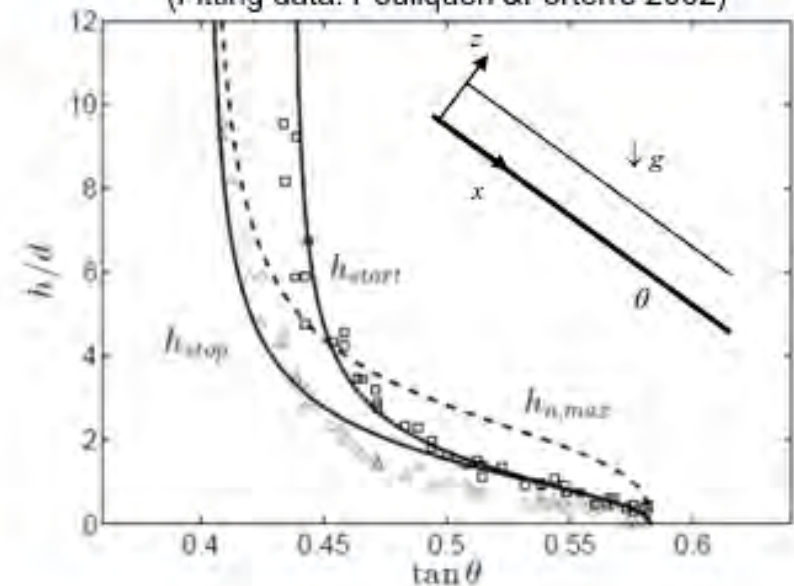
Application to uniform incline flow

(Fitting data: Pouliquen & Forterre 2002)

- h_{start} and h_{stop} phenomenon

$$h_{\text{stop}}(\theta) \approx \frac{\pi}{2} \frac{\zeta}{\sqrt{r(\theta) - r(\mu^*)}}$$

$$h_{\text{start}}(\theta) \approx \frac{\pi}{2} \frac{\zeta}{\sqrt{r(\theta)}}$$



- In the **thick-layer limit**,

Predicted mean flow property

$$\bar{u} = (\pi\zeta/5d)\sqrt{\rho g h \cos \theta} (h/h_{\text{stop}}),$$

=

Pouliquen flow rule (1999)

$$\bar{u}/\sqrt{gh} = \beta h/h_{\text{stop}}$$

because of the following scaling equivalence:

$$\rho g h \sim \rho h_{\text{stop}}^2 (\bar{u}/h)^2 \longrightarrow \tau \sim \rho l^2 \dot{\gamma}^2$$

$h_{\text{stop}} \sim$ Correlation length

(Ertas & Halsey 2002; GDR midi 2004; Staron 2008; Baran et al. 2006)

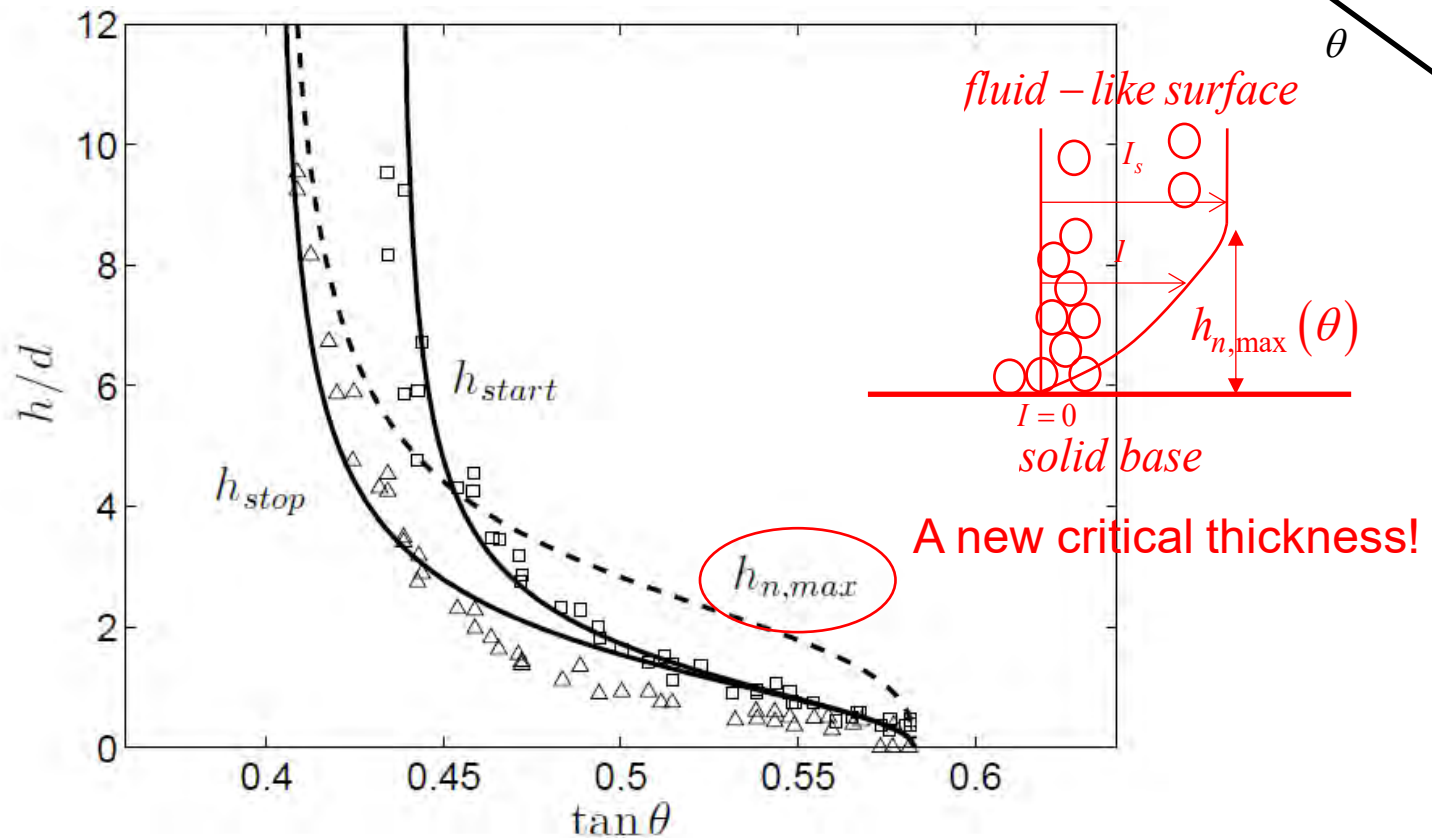
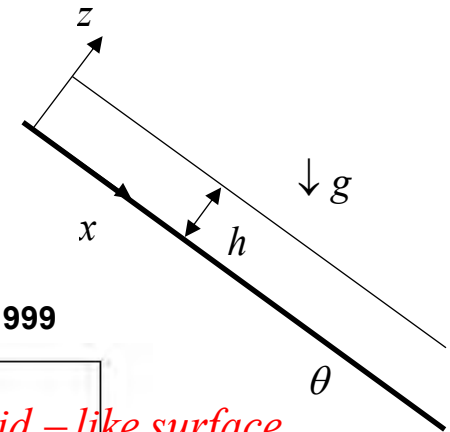
Application to gravity-driven inclined flows

■ Hysteresis critical thickness.

At a specific angle θ ,

- Static pile \rightarrow Flow, when $h > h_{\text{start}}$
- Flow \rightarrow Static pile, when $h < h_{\text{stop}}$

Pouliquen 1996, 1999; Daerr & Douady 1999

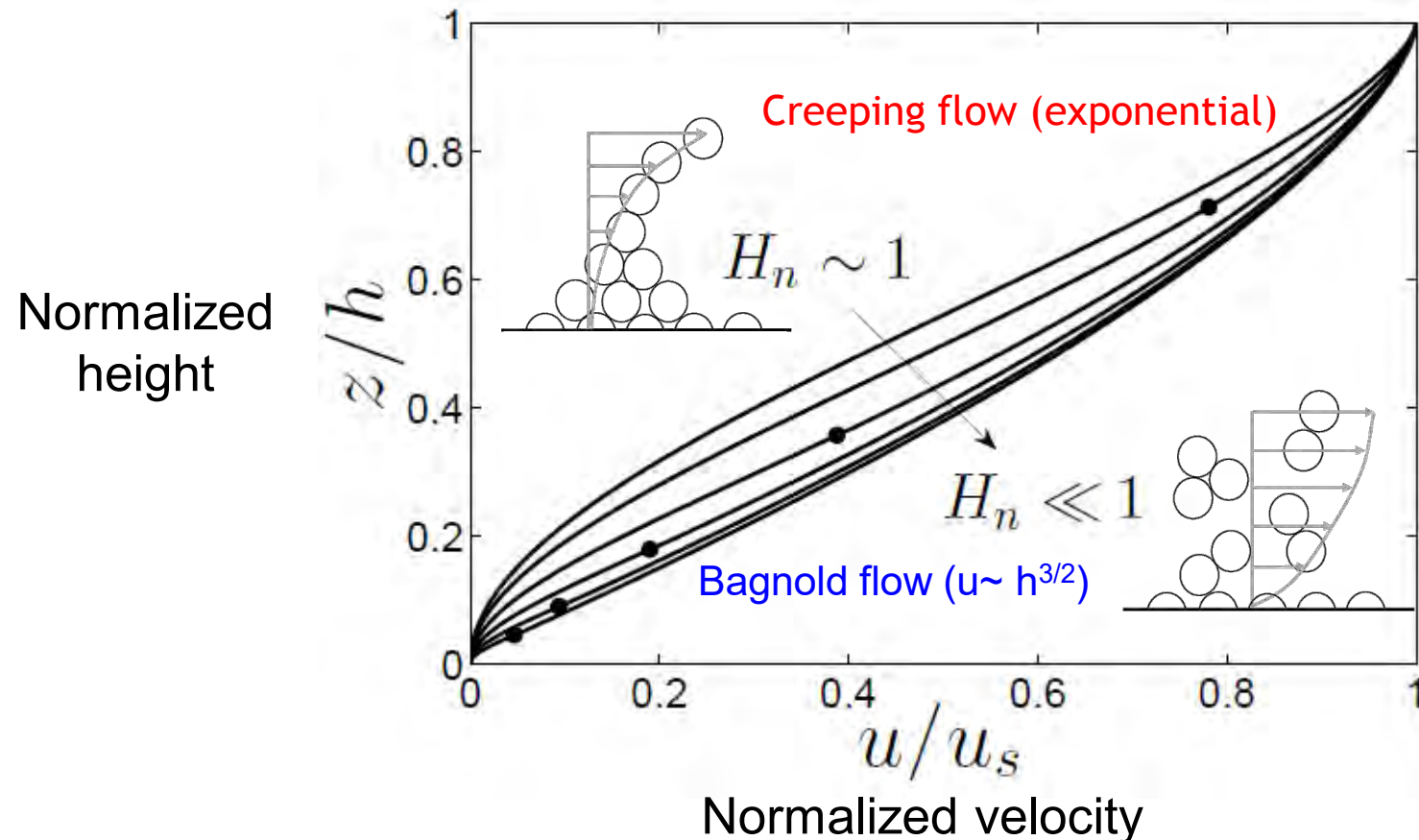
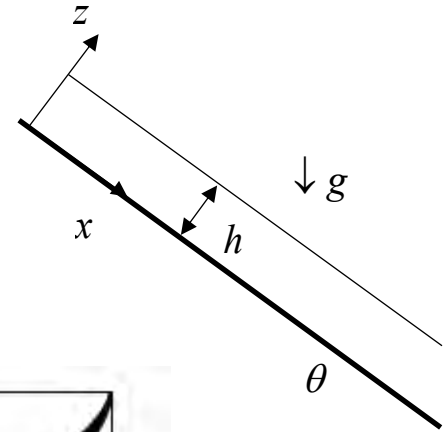


The data are extracted from Forterre & Pouliquen 2002

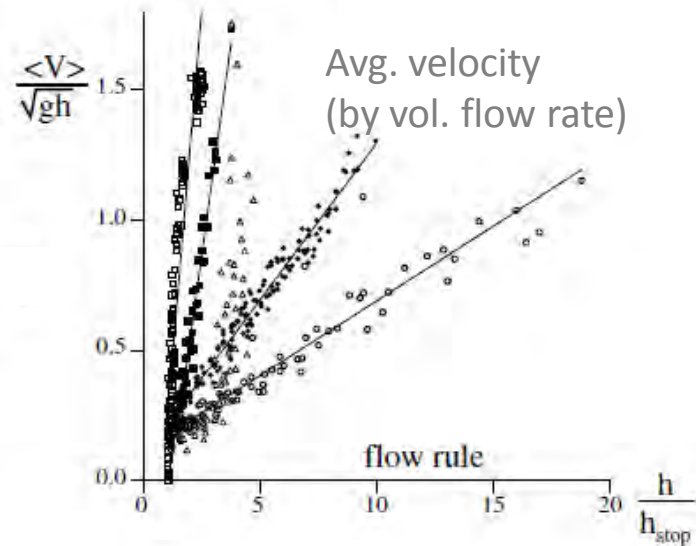
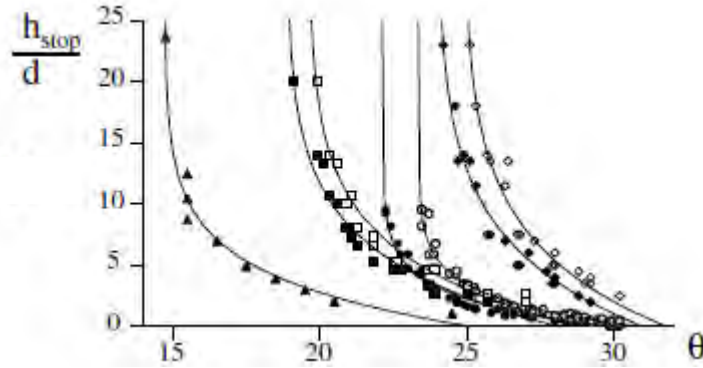
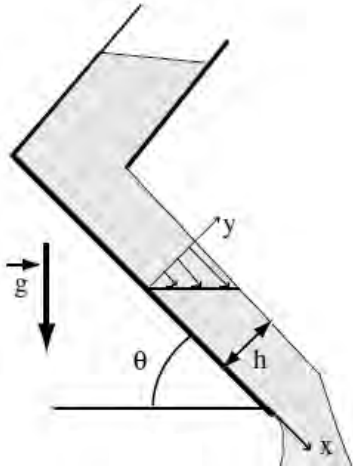
Application to gravity-driven inclined flows

■ Creeping and Bagnold flow velocity profiles

- Non-local parameter: $H_n \equiv h_{n,\max}(\theta)/h$
- Observed in DEM (Silbert et al 2003)



2D Inclined Free surface



Empirical models:

$$\theta_{stop} \sim fn\left(\frac{h_{stop}}{d}\right)$$

$$\frac{\langle V \rangle}{\sqrt{gh}} = \alpha + \beta \frac{h}{h_{stop}(\theta)}$$

$$\Rightarrow \theta_{stop} = fn\left(\frac{d}{h_{stop}}\right) = \frac{\|U\| d}{\sqrt{gh} h} - \alpha \frac{d}{h}$$

At equilibrium, $Tan(\theta_{stop}) = \mu_{eff}$

